Transworld Research Network
37/661 (2), Fort P.O., Trivandrum-695 023, Kerala, India

Recent Res. Devel. Sound & Vibration, 1(2002): 29-61 ISBN: 81-7895-031-6

Nonlinearly damped oscillators

José L. Trueba, José P. Baltanás and Miguel A. F. Sanjuán
Nonlinear Dynamics and Chaos Group, Departamento de Ciencias Experimentales e Ingeniería,
Universidad Rey Juan Carlos, Tulipán s/n, 28933 Móstoles, Madrid, Spain

Abstract

Nonlinear damping terms proportional to the power of the velocity are considered, and their effect on different aspects of the dynamics of some nonlinear oscillators is throroughly discussed. We use analytical methods and extensive numerical simulations, in order to gain a better understanding of the role played by the nonlinear friction. We have observed how it affects the fractal basin boundaries, the threshold of period-doubling route to chaos and the erosion of the basin structure. Analytical expressions giving specific information on the threshold for the homoclinic bifurcations to occur are also offered. Furthermore, we apply the notion of Melnikov-equivalence to nonlinearly damped oscillators, as a way to establish relations among them. And finally a general

Correspondence/Reprint request: Dr. Miguel A. F. Sanjuán, Nonlinear Dynamics and Chaos Group, Escuela Superior de Ciencias Experimentales y Tecnología, Universidad Rey Juan Carlos, 28933 Móstoles, Madrid, Spain.
Tel: +34 916647443, Fax: +34 916647490, E-mail : msanjuan@escet.urjc.es

discussion on how the energy dissipates as a function of time and over a cycle is presented.

Introduction

Nonlinear oscillators have played an important role in the study of physics and natural phenomena since old. In particular, they have deserved much attention as a paradigm in order to analyze all kind of phenomena related to oscillations, bifurcations and chaos; it is also well known their paradigmatic importance in mathematics [1]. Their interest derives not only from their intrinsic value as notable examples to test and search for new phenomena, but also for their wide range of applicability. We can cite mechanics and mechanical engineering [2], condensed matter physics [3], celestial mechanics [4], biology [5], economy and social sciences [6] as some fields of application of nonlinear oscillators.

It is well known that most oscillatory systems are subject to some kind of damping in practice. A discussion of damping in the context of nonlinear dynamics appears for example in [7]. The dissipative forces that cause this damping may act on a system in the form of dry friction, such as Coulomb friction, which is typically a nonlinear damping mechanism, drag or aerodynamic friction, which is typically proportional to the square of the velocity and viscous forces which are linear in the velocity. Furthermore, it is usual to find in practical applications very complex frictional and drag forces, in these cases, power-law terms in the velocity are used to model the real frictional forces, which are experimentally determined with the use of wind tunnels or water tanks. Among the possible models, one of the simplest empirical mathematical model of the dissipative force is taken as $f(v) \propto -v\,|v|^{p-1}$,Where v represents the velocity, with its positive or negative sign, and $p \geq 0$. Notice that the absolute value of the velocity is needed to safeguard the fact that the dissipative force must be contrary to the motion of the system. Moreover $f(v)$ is an odd function of v, $f(-v) = f(v)$. Taking this fact into account one can recover from this expression the important cases of Coulomb damping ($p = 0$), linear viscous damping ($p = 1$), and draglike friction ($p = 2$). A historical review of the applications of the Coulomb damping can be found in [8], and a good treatment of the case $p = 1$ and its applications may be found in [7,9]. Phenomenological models accounting for nonlinear dissipation forces with higher values of p have been considered in some applied sciences, such as ship dynamics, sound and vibration engineering, and motion of projectiles, among others [10-17]. As a matter of fact, a physical interpretation of these higher order damping terms may be given by assuming a power series expansion on the velocity of more complicated damping forces.

Most systems are subject to a different combination of terms of damping, each one of them with different effects. Taking into account the above considerations, this fact naturally leads to consider a function of the form

$$D(\dot{x}) = \sum_{i=1}^{N} b_{p_i} \dot{x} |\dot{x}|^{p_i - 1} \tag{1}$$

($b_{p_i} > 0$) as a sufficiently general damping function. Particular cases of this equation, including combinations of linear plus quadratic damping terms, linear plus cubic damping

terms or even combinations of linear plus quadratic plus cubic terms have been considered in [13] in the context of the naval architecture literature. Nonlinear damping also plays an important role in other applied systems since it may be used to supress large amplitude oscillations or various instabilities, and it can be also used as a control mechanism. The effect of some physical parameters, such as wave amplitude and nonlinear damping, on the transient motions and the global system behaviour of a capsizing ship was investigated in [14]. In particular they use a model of a double-well and a single-well Duffing oscillator with a linear plus a quadratic damping term. The stability of a nonlinearly damped hard Duffing oscillator was analyzed in [10], and the role of nonlinear dissipation in soft Duffing oscillators in [11], with the main result that the threshold value necessary to generate period-doubling shifts backwards as the damping exponent increases. Moreover in [12] it was shown that nonlinear damping could be used as a mechanism to suppress chaos. The effect of nonlinear dissipation on some properties of the dynamics of the universal escape oscillator, such as the threshold of period-doubling bifurcations, fractal basins boundaries and the destruction of the basins of attraction was considered in [18], and some analytical estimates of the nonlinear damping effects for the Duffing oscillator and for the pendulum, using Melnikov techniques, in [19]. Moreover, the effect of nonlinear damping in the energy dissipation of a double-well Duffing oscillator is investigated in [20], concluding that different terms of damping lead to different ways of energy dissipation, though some general features are common to all these nonlinearly damped Duffing oscillators. A rather interesting example of application of nonlinear damping appears in [21] in the context of dissipation in barred galaxies and the analysis of the mechanisms by which mass concentrations are produced, where a model of a quadratically damped pendulum is used. As a matter of fact, dynamical friction of this sort is common in galactic dynamics [22].

All nonlinear oscillators models analyzed here are periodically forced oscillators, where the forcing is considered to be a harmonic function, that is, a trigonometric function, Nonharmonic periodic forcing by using Jacobian elliptic functions and its effects on the dynamics of some nonlinear oscillators have been discussed in [23-25]. One of the interesting mechanisms introduced by the nonharmonic perturbations is the consideration of the shape and wave form of the driver. Furthermore it is interesting to note that a Lagrangian and a Hamiltonian formulation is possible, and in particular for linearly damped nonlinear oscillators is given in [26].

The structure of this paper is the following. In section II, we discuss the effect of including nonlinear damping terms in the equations of motion of the nonlinearly damped universal escape oscillator, showing different quantitative effects on its dynamics. Section III is devoted to the application of the Melnikov method, in order to investigate analytically the effect of nonlinear friction terms in the cases of the universal escape oscillator, the Duffing oscillator and the simple pendulum. In section IV, the concept of Melnikov-equivalent systems is used to give a quantitative understanding of different damped oscillators. As a conclusion, it is shown that a relation between different damping terms is possible and can be performed in practical cases. But this is not all, because other dynamical effects have to be taken into account if we try to relate different ways of damping: in particular, the question of the energy dissipation. An intensive treatment of this problem is done in section V, showing that, from the energetic point of view, different damping terms can not be treated as equivalent. Finally, the conclusions are described in section VI.

2. Relevance of nonlinear damping in the dynamics of nonlinear oscillators

Numerous physical phenomena of oscillatory nature appearing in different fields present the ability to escape from a potential well, and are described by a universal escape nonlinear oscillator model. This nonlinear oscillator has a simple mechanical interpretation, since it describes the motion of a particle of unit mass in the cubic potential $V(x) = x^2/2 - x^3/3$ sinusoidally driven, and which is considered as a prototype for escape phenomena. When a linear dissipative force is introduced, its equation of motion is

$$\ddot{x} + b\dot{x} + x - x^2 = F \sin \omega t, \tag{2}$$

where b is the damping coefficient, F the forcing amplitude and ω the frequency of the external perturbation.

Our hypothesis in this section is the following: the introduction of nonlinear damping terms in the laws of motion of a nonlinear oscillator affects quantitatively the behavior of the system. To motivate this hypothesis, in this section we perform some numerical experiments on the universal escape oscillator. Even though some authors [28,31] mention the possible interesting role played by considering nonlinear damping terms, they only contemplated linear damping. A comprehensive study of the effect of including nonlinear damping terms on the dynamics of this nonlinear oscillator was carried out by Sanjuán [18]. In that work an analysis of the bifurcation diagrams and the erosion patterns of the basins of attraction was presented, following some of the ideas reported in [33].

The equation of motion for the sinusoidally driven escape oscillator including a nonlinear damping term proportional to a power of the velocity, with coefficient $b_p \geq 0$ and exponent $p \geq 0$, reads

$$\ddot{x} + b_p \dot{x} \, |\dot{x}|^{p-1} + x - x^2 = F \sin \omega t, \tag{3}$$

where F and ω the forcing amplitude and the frequency of the external perturbation respectively. Note that we consider here a particular case of the more general nonlinear damping force introduced in the previous section. The general case will be consider later, when we introduce the idea of Melnikov-equivalent damped oscillators.

The dynamics of the escape oscillator has been simulated using a fixed-step-size fourth order Runge-Kutta numerical integration and its associated two-dimensional Poincaré map. We want to analyze the main features of the steady solutions of the system for different values of p. As in [33], for most of our numerical computations we use a fixed frequency $\omega = 0.85$ and a damping level $b_p = 0.1$ and when we modify the damping exponent p, we observe that the basins erose strongly as the damping parameter p increases. The effect is similar to keeping fixed all parameters and decreasing the forcing term. For $p = 1$ and for the initial condition (0.175, –0.55), which is close to a fixed point attractor, a nice Feigenbaum period-doubling cascade in the forcing parameter range $0.1 \leq F \leq 0.109$ is found (this corresponds to the result shown in [29,30]). When a quadratic nonlinear damping is used, that is $p = 2$, and for the same initial condition as before, a

chaotic cascade in the parameter range $0.087 \leq F \leq 0.096$ appears, which is shown in Fig. 1. One of the effects of using the quadratic nonlinear damping is precisely the lowering of the critical forcing for which the homoclinic bifurcation and the escape boundary take place. In particular for $F = 0.0954$, the result is a beautiful two piece chaotic attractor with a Lyapunov dimension $D_L = 1.22$. This chaotic attractor is shown in Fig. 2, where both pieces of the attractor are clearly seen.

When $p = 3$, that is a cubic nonlinear damping, chaotic solutions are found as well in the parameter region $0.083 \leq F \leq 0.093$. Consequently it appears to be a shift backwards in the period-doubling bifurcation threshold and escape as the damping exponent p is increased. If our numerical experiments are compared to the results shown for the linear damping case ($p = 1$) in [33] we may conclude that increasing the damping exponent p has similar effects as decreasing the damping coefficient b_p.There is a rather intuitive argument to justify this behaviour. Think for simplicity in a particle moving with certain energy inside the potential well. Using topological arguments concerning the phase space of the escape oscillator, the velocity $\dot{x}(t)$ is bounded and $|\dot{x}(t)| < 1$ for all times, for any motion inside the potential well. This being so, it implies that $|\dot{x}(t)|^p < |\dot{x}(t)| < 1$, for $p > 1$. So this explains intuitively the observations of the numerical experiments carried out for different values of the damping exponent, since using a parameter $p > 1$ implies a reduction of the damping term which numerically is

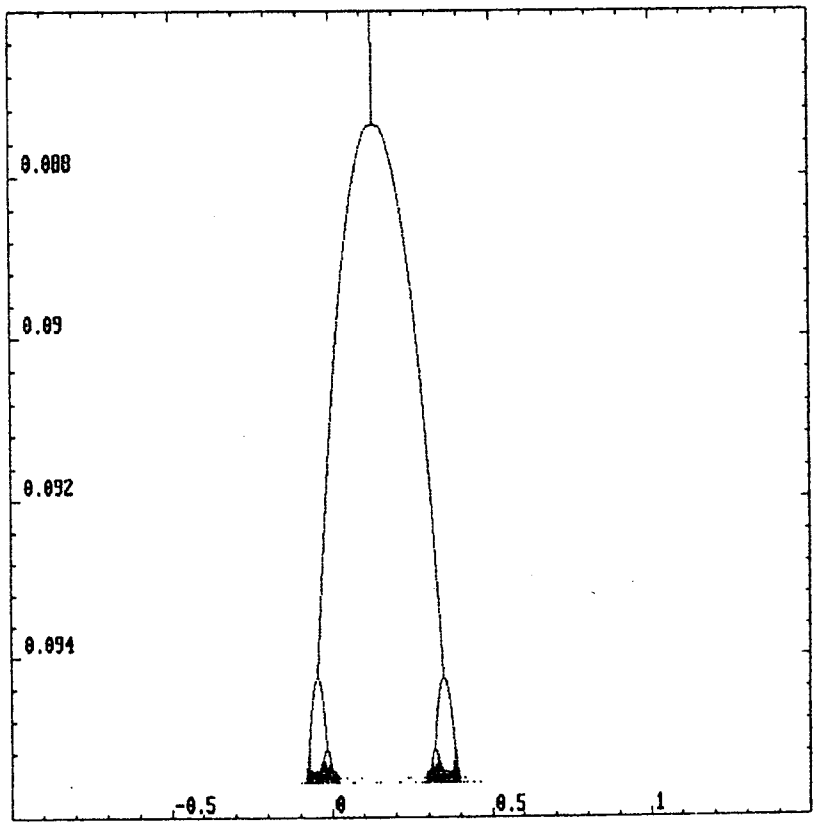

Figure 1. Plot of the period-doubling bifurcation diagram of the quadratically damped universal escape oscillator $\ddot{x} + 0.1\dot{x}|\dot{x}| + x - x^2 = F \sin 0.85t$ for the initial condition (0.175, −0.55). The parameter F runs over the interval $0.086 < F < 0.096$.

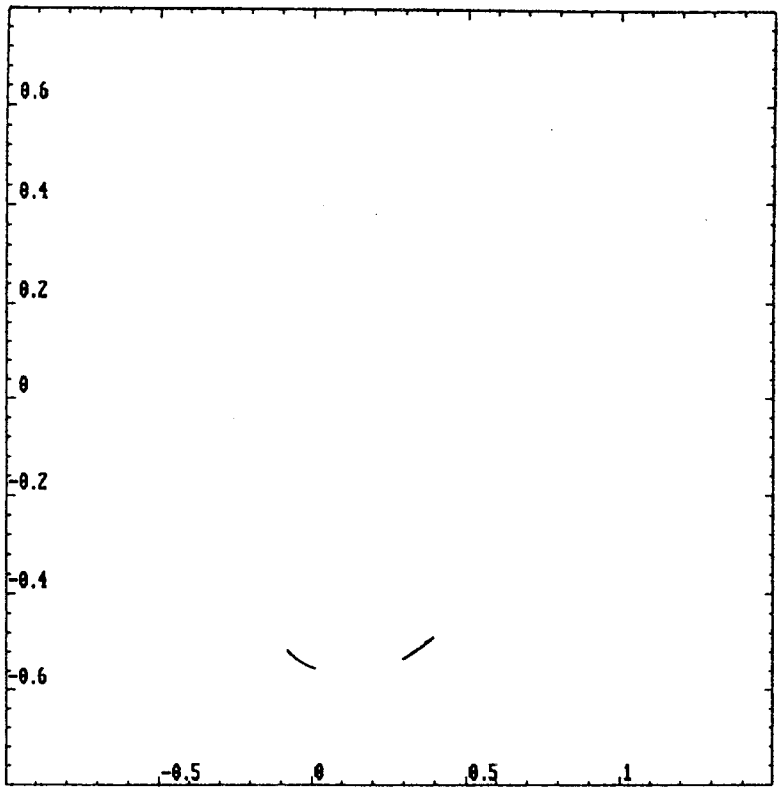

Figure 2. Two-piece chaotic attractor of the quadratically damped universal escape oscillator $\ddot{x} + 0.1\,\dot{x}\,|\,\dot{x}\,| + x - x^2 = 0.0954 \sin 0.85t$ for the initial condition (0.175, –0.55). Its Lyapunov dimension is 1.22.

equivalent to using the linear damping term with a lower damping level.

A basin of attraction is defined as the set of points that taken as initial conditions are attracted to a fixed point or an invariant set (see e.g. [35,36]). As it was mentioned previously, the escape oscillator may be seen as a mechanical oscillator where a particle of unit mass moves inside an assymetrical potential well, with the possibility of escape. This means that besides the possible attractors that may coexist in the interior of the well, the infinity may be taken as an attractor as well. The basin of attraction in this case signals the points in phase space that are attracted to a safe oscillation within the potential well, and the set of points that escape outside the potential well to the infinity. A study of these basins of attraction for the escape oscillator has been done extensively and with considerable detail by Michael Thompson and collaborators in a series of papers [29-34]. What we want to study now is the effect of using nonlinear damping terms on the equation of the escape oscillator and how the basins of attraction are affected as the damping exponent p is increased. We follow two strategies. The first one consists in fixing the forcing amplitude $F = 0.05$ and then to compute the basins of attraction for different damping exponents, that is, linear damping, quadratic damping and cubic damping for three different sets of damping coefficients at $b = 0.1$, $b = 0.15$ and $b = 0.2$. To numerically generate the basins of attraction, we select a grid of 300 × 300 points in the region of phase space determined by the rectangle of points (–0.8, 1.4) × (–0.8, 0.8), which are taken as initial conditions. Depending to which attractor an initial point goes, it

is assigned a different color. Those initial points which go to any attractor located in the interior of the well are assigned the color white. The color black is assigned to any initial point which escapes the potential well. These computations are shown in Fig. 3. The first column shows the basins of attraction for a fixed value of the damping level, $b = 0.1$, the second column corresponds to $b = 0.15$ and the third column to $b = 0.2$. On the other hand the first row corresponds to damping exponent $p = 1$, that is, linear damping, the second row to $p = 2$, quadratic nonlinear damping, and the third row to $p = 3$, cubic nonlinear damping. Observing these basins of attraction in Fig. 3 it is infered that for a fixed damping level, the increase of the damping exponent, has a clear effect on the destruction of the safe areas inside the well and the erosion of the basins increases notably. If we compare these results to the corresponding results for linear damping for which only the damping level is varied, the conclusion is that they are equivalent to a decrease of the damping level.

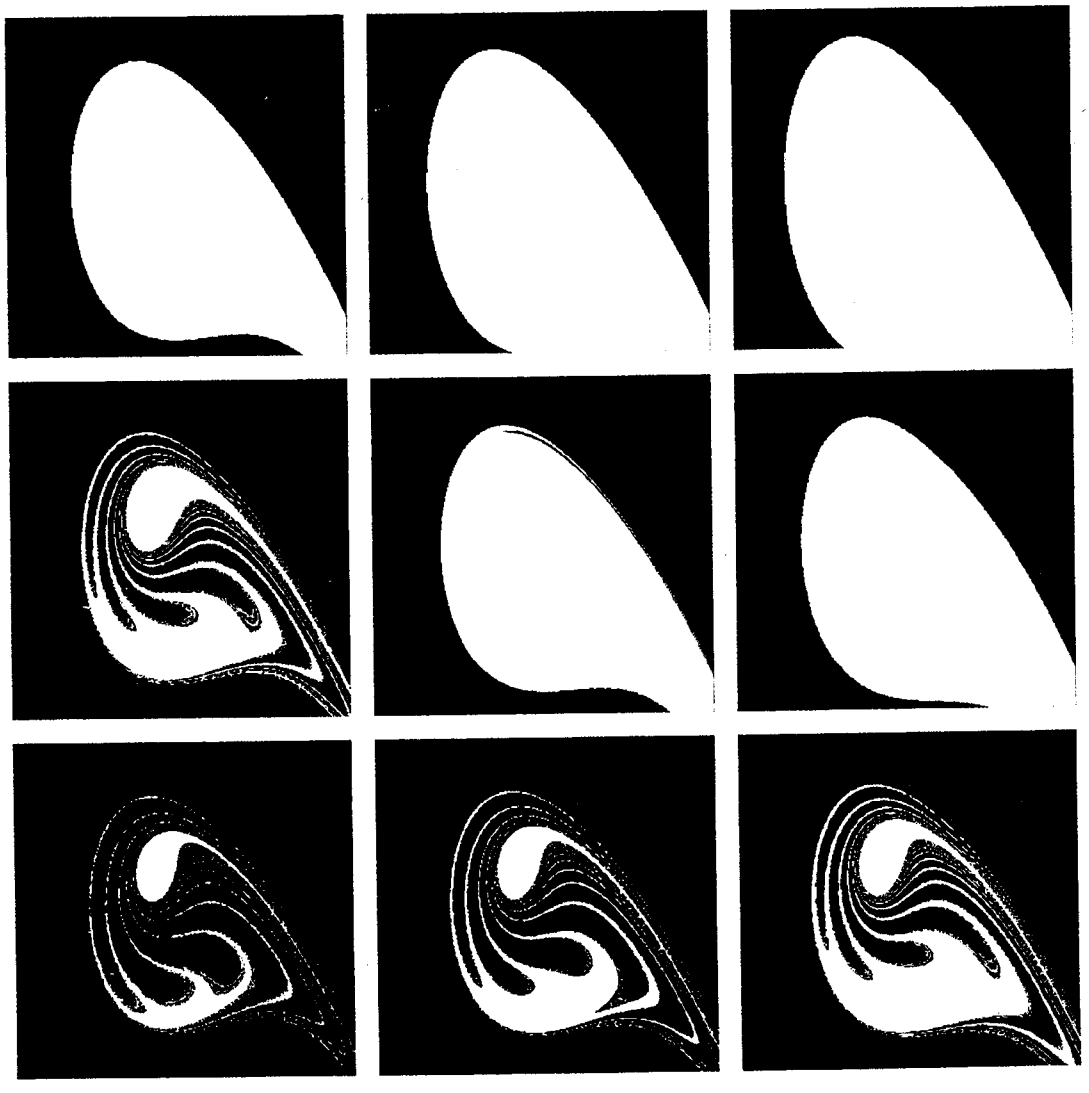

Figure 3. Basin erosion pattern of the escape oscillator $\ddot{x} + b_p\dot{x}|\dot{x}|^{p-1} + x - x^2 = 0.05 \sin 0.85t$. The first column corresponds to $b_p = 0.1$, the second to $b_p = 0.15$ and the third to $b_p = 0.2$. The first row corresponds to $p = 1$, the second to $p = 2$ and the third to $p = 3$.

The second strategy is fixing the damping coefficient at $b = 0.1$ and considering different values of forcing amplitudes such as $F = 0.03$, $F = 0.05$ and $F = 0.07$ for the linear, quadratic and cubic dampings. The first column of Fig. 4 shows the basins of attraction for $F = 0.03$, the second column corresponds to $F = 0.05$ and the third column to $F = 0.07$. The rows correspond to linear, quadratic and cubic damping respectively. The basins in this figure show that indeed the damping exponent has a strong effect on the erosion of the basin, but the strongest effect is manifested by the increase of the forcing as it happens as well in the linear damping case.

In some of these basins shown in Fig.3 and Fig.4 two attractors coexist in absence of any kind of fractalization of the boundaries. Something interesting to mention concerning most basins shown here is the presence of very clear basin cells [35-39]. The notion of trapping region clarifies this idea. A trapping region is a region in phase space from which points cannot escape. Once the trajectory enters this region cannot leave it and also there must be at least one attractor located there. A cell is a region in phase space

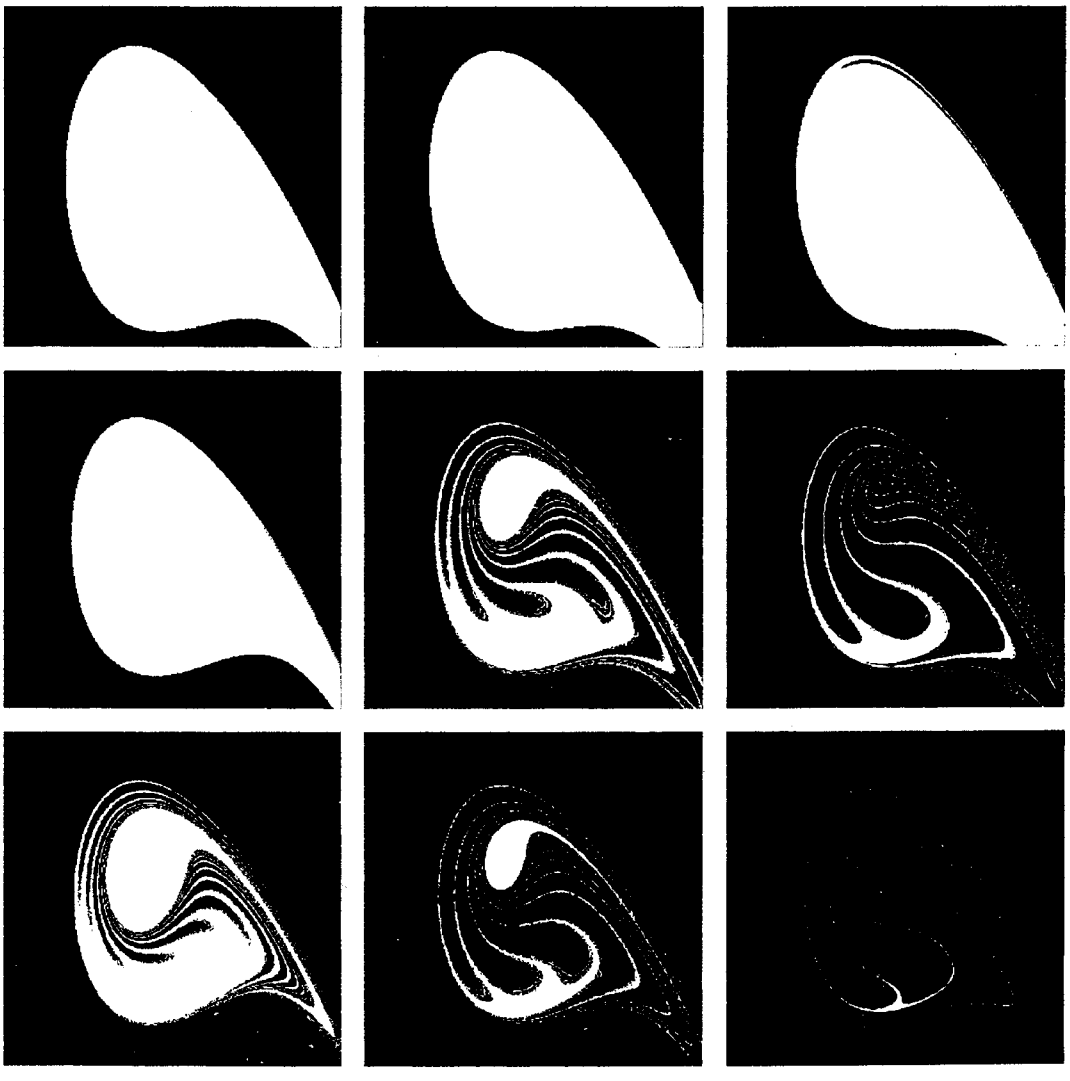

Figure 4. Basin erosion pattern of the escape oscillator $\ddot{x} + 0.1\dot{x}|\dot{x}|^{p-1} + x - x^2 = F\sin 0.85t$. The first column corresponds to $F = 0.03$, the second to $F = 0.05$ and the third to $F = 0.07$. The first row corresponds to $p = 1$, the second to $p = 2$ and the third to $p = 3$.

whose boundary consists of pieces of the stable and unstable curves of some periodic trajectories. When a cell is a trapping region then is a basin cell. One of these basin cells is shown crosshatched in Fig. 5, and corresponds to $p = 3$, $b = 0.1$ and $F = 0.03$. A period 1 orbit which generates the basin cell, which is situated at the coordinates (0.092, 0.425) and the boundaries are its associated stable and unstable manifolds.

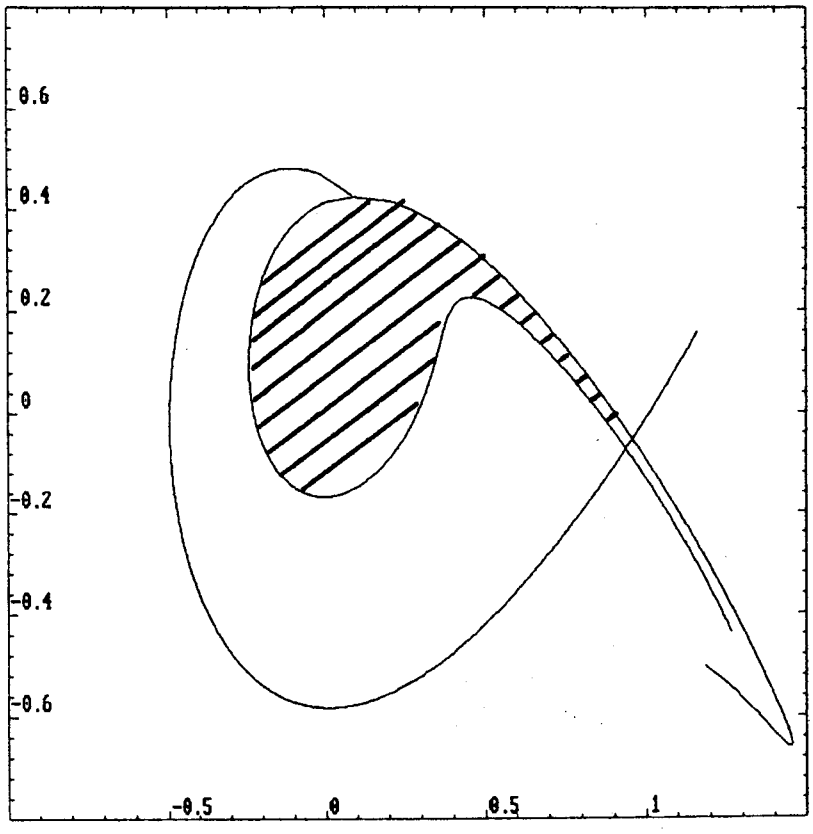

Figure 5. A basin cell, crosshatched, of the cubic damped universal escape oscillator $\ddot{x} + 0.1\dot{x}^3 + x - x^2 = 0.03 \sin 0.85t$ generated by a period 1 orbit situated at (0.092, 0.425).

3. Melnikov method for nonlinearly damped oscillators

Numerical experiments done in the previous section have shown that when a nonlinear damping term is used instead of a linear damping term the global pattern of bifurcations is clearly affected. Even though only the universal escape oscillator has been used for these numerical computations, similar results appear in the case of the Duffing oscillator or the simple pendulum. Now we will try to recover these results using the Melnikov method, which is one of the few analytical tools to study the global bifurcation behavior of nonlinear systems. A good introduction about the Melnikov method is found in [40], and a physical interpretation is provided by Ketema in [41]. As is well known, this technique is a first-order perturbative method which gives the condition for the crossing of the stable and unstable manifolds, that is to say, this does not mean that what we have is *permanent chaos*, but a horseshoe type dynamics associated to the phenomenon of *transient chaos*. Although the chaos does not manifest itself in the form of permanent chaos, it does in terms of the fractal basin boundaries, as was shown by

Moon and Li [42].

In the present section, we analyze the universal escape oscillator, the double-well Duffing oscillator and the simple pendulum. From a quantitative point of view, some properties of the chaotic invariant set are indeed modified when the nonlinear damping terms are included. This clearly shows a manifest and quantitative effect of the nonlinear dissipation on the dynamics of the strange attractor. The role of these effects is studied by introducing, in the next section, a generalized nonlinear damping term, and by using the concept of Melnikov-equivalent systems, introduced in [13] and developed in [19].

A.The nonlinearly damped universal escape oscillator

In absence of forcing and damping this system is completely integrable. In order to apply the Melnikov method, the first step is the computation of the hyperbolic fixed points of the unperturbed system

$$\ddot{x} + x - x^2 = 0. \tag{4}$$

This system has an hyperbolic fixed point at (1,0). So it has a separatrix orbit (homoclinic orbit) in phase space, which divides it into two regions, one of bounded motions and one of unbounded motions. Only the points inside the separatrix correspond to bounded motions and the inclusion of a external perturbation makes it possible the possibility of escape to infinity. Next we have to compute this homoclinic orbit, that is, the solution of the unperturbed system starting and ending at the hyperbolic fixed point. This implies to integrate the equations of motion from the initial condition (−1/2,0), which belongs to the homoclinic orbit because it has the same energy as the hyperbolic fixed point. The equations of motion of the separatrix orbit of the unperturbed system are

$$x_s(t) = \frac{3}{2}\tanh^2\left(\frac{t}{2}\right) - \frac{1}{2}, \tag{5}$$

$$y_s(t) = \frac{3}{2}\tanh\left(\frac{t}{2}\right)\operatorname{sech}^2\left(\frac{t}{2}\right). \tag{6}$$

According to Melnikov theory we need the previous ingredients in order to calculate the Melnikov function, which is associated to each homoclinic orbit. This function is calculated through the expression

$$M(t_0,\omega,p) = -b_p\int_{-\infty}^{+\infty}|y_s(t)|^{p+1}\,dt + F\int_{-\infty}^{+\infty} y_s(t)\sin\omega(t+t_0)dt. \tag{7}$$

After substitution of the homoclinic solutions, where the Melnikov function need to be evaluated, it appears as

$$M(t_0,\omega,p) = -\left(\frac{3}{2}\right)^{p+1} b_p\int_{-\infty}^{+\infty}\left|\tanh\left(\frac{t}{2}\right)\right|^{p+1}\operatorname{sech}^{2(p+1)}\left(\frac{t}{2}\right)dt \tag{8}$$

$$+\frac{3}{2}F\cos\omega t_0\int_{-\infty}^{+\infty}\tanh\left(\frac{t}{2}\right)\operatorname{sech}^2\left(\frac{t}{2}\right)\sin\omega t\;dt. \tag{9}$$

After evaluating the integrals (See Appendix A),

$$M(t_0,\omega,p) = -2\left(\frac{3}{2}\right)^{p+1} b_p B\left(\frac{p+2}{2}, p+1\right) + \frac{6\pi\omega^2 F}{\sinh(\pi\omega)}\cos\omega t_0. \tag{10}$$

In this equation appears the function $B(r,s)$, which is the Euler Beta function and it can be easily evaluated in terms of the Euler Gamma function [43].

The Melnikov function is related to the distance between the stable and the unstable manifolds associated to the hyperbolic fixed point, when destroyed by the perturbation. When this function has simple zeros, it implies that there is a critical parameter F_{cp} corresponding to the external forcing, for which homoclinic tangles intersect. For a certain frequency ω this critical parameter depends on the damping exponent p and the damping coefficient b_p. This critical parameter may be written as

$$F_{cp} = b_p \frac{3^p}{2^{p+1}\pi\omega^2} B\left(\frac{p+2}{2}, p+1\right)\sinh(\pi\omega). \tag{11}$$

We define the function $R(\omega,p) = F_{cp}/b_p$, as the ratio between the external forcing and the damping coefficient and then we have the following expression

$$R(\omega,p) = \frac{3^p}{2^{p+1}\pi\omega^2} B\left(\frac{p+2}{2}, p+1\right)\sinh(\pi\omega). \tag{12}$$

This last function is the one that provides information about the effect of the nonlinear damping on the threshold of homoclinic chaos and the appearance of fractal boundaries. Accordingly, given a set of parameters of the system we may know when it is expected to find chaotic behavior in its dynamics. A similar analysis to the one described here, for linear damping terms, and for periodic and quasiperiodic perturbations was carried out in [27], where the homoclinic bifurcations for each case were computed and classified.

In order to have a visual information about this last result, we have plotted in Fig.6 the dependence of the ratio $R(\omega,p)$ with respect to the damping exponent p for the above used value $\omega = 0.85$ of the frequency of the external forcing. This figure shows a decaying dependence of the Melnikov ratio with p. Hence when a nonlinear damping term is used instead of linear damping term, with a fixed damping coefficient b_p, then the critical forcing for fractal basin boundaries to occur decreases. In the case of linear damping, $p = 1$, the Melnikov ratio is given by $R(\omega,1) = \sinh(\pi\omega)/5\pi\omega^2$ and the critical forcing, when $\omega = 0.85$, is $F = 0.633 \times \alpha_p$, which is the expression obtained in [29,30]. The critical forcing terms for the quadratic and cubic nonlinear damping, with $b_p = 0.1$, have been explicitely calculated. Its values are $F = 0.0297$ for the quadratic case and $F = 0.0148$ for the cubic case. These findings confirm the results obtained with the help of numericals tools, that is, the onset of chaos shifts backwards as the damping exponent p is increased. This critical forcing gives the threshold for the fractal basin boundaries to appear. Moreover, for these critical values the invariant manifolds associated to the fixed point of saddle type of the Poincaré map associated to the escape oscillator, intersect themselves tangentially. Figure 7 (left) shows the tangency of the unstable (the inset) and stable (the outset) manifolds associated to the saddle fixed point situated at (0.999,

–0.015), for $F = 0.0297$ and $\omega = 0.85$, with quadratic nonlinear damping. The homoclinic tangency for the invariant manifolds associated to the saddle fixed point at (0.999, –0.007) for $F = 0.0148$ and $\omega = 0.85$ is shown in the Figure 7 (right), when a cubic

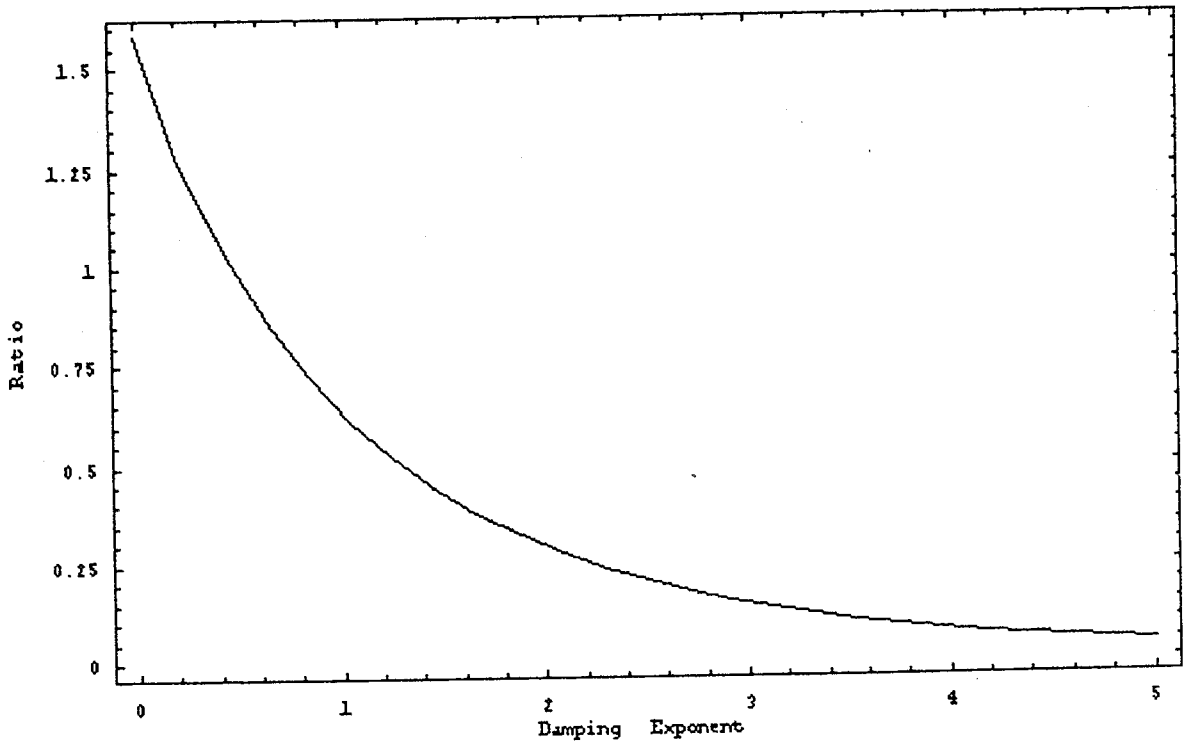

Figure 6. Dependence of the function $R(\omega, p)$ with respect to the damping exponent p for $\omega = 0.85$.

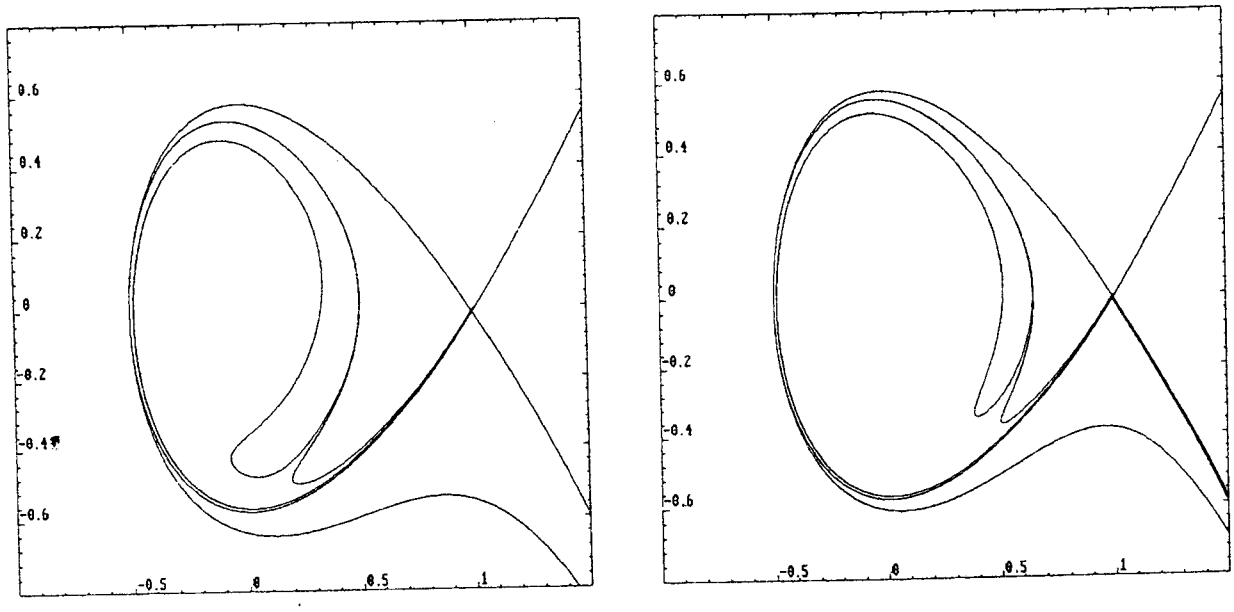

Figure 7. Homoclinic tangency for two different nonlinearly damped universal escape oscillators, as calculated with the help of Melnikov method. (Left) Quadratically damped universal escape oscillator with $p = 2$, $b_2 = 0.1$, $\omega = 0.85$ and $F = 0.0297$. (Right) Cubic damping term with $p = 2$, $b_3 = 0.1$, $\omega = 0.85$ and $F = 0.0148$.

nonlinear damping is considered. The inset is the unstable manifold and the outset is the stable manifold.

B. The nonlinearly damped double-well Duffing oscillator

One of the models of nonlinear oscillators that traditionally has received much attention in the literature is the Duffing oscillator. Besides its multiple applications in many different fields, it constitutes also a paradigm in the study of nonlinear oscillations. For this reason we consider the following equation of motion for the driven double-well Duffing oscillator with a nonlinear damping term

$$\ddot{x} + b_p \dot{x} \, |\dot{x}|^{p-1} - x + x^3 = F \cos \omega t, \tag{13}$$

where F is the amplitude and ω the frequency of the external perturbation, and analyze how it affects its dynamics. A similar model was used previously by Ravindra & Mallik in [10,11] to study the role of nonlinear damping on some soft Duffing oscillators.

Our purpose here is, as in the case of the universal escape oscillator, to analytically estimate certain effects of nonlinear damping terms in the dynamics of this nonlinear oscillator. Extensive numerical experiments of the kind previously described for the universal escape oscillator, have given evidence that modifying the damping exponent has a considerable effect on the global pattern of bifurcations. In order to carry this analytical study out, we will make use of the Melnikov techniques again. As this method states, we need to consider the external forcing and the dissipation as small perturbations to the Hamiltonian system $\ddot{x} - x + x^3 = 0$. A corresponding Melnikov analysis for the linearly damped double-well Duffing oscillator, $p = 1$ in our model, may be found in [40]. As above, one basic step for the application of the method is the calculation of the fixed points in phase space of the unperturbed integrable system. This system has tow elliptic fixed points located at (±1,0) and a hyperbolic fixed point located at (0,0). The homoclinic orbits, that is, the solutions of the unperturbed system starting and ending at the hyperbolic fixed point, can be found by integrating the system for the initial conditions $(\pm\sqrt{2}, 0)$, giving

$$x_s^{\pm}(t) = \pm\sqrt{2} \operatorname{sech} t, \tag{14}$$

$$y_s^{\pm}(t) = \mp\sqrt{2} \operatorname{sech} t \tanh t, \tag{15}$$

where the signs refer to the right and left half planes. Both solutions determine the separatrix orbit, since it separates two types of orbits in phase space.

The Melnikov function associated to this separatrix then gives

$$M^{\pm}(t_0, \omega, p) = -2^{\frac{p+1}{2}} b_p \int_{-\infty}^{+\infty} \operatorname{sech}^{p+1} t \, \tanh^{p+1} t \, dt \tag{16}$$

$$\mp\sqrt{2} F \sin \omega t_0 \int_{-\infty}^{+\infty} \operatorname{sech} \quad \tanh t \sin \omega t \, dt. \tag{17}$$

$$M^{\pm}(t_0,\omega,p) = -b_p 2^{\frac{p+1}{2}} B\left(\frac{p+2}{2},\frac{p+1}{2}\right) \pm F\sqrt{2}\pi\omega \operatorname{sech}\left(\frac{\pi\omega}{2}\right)\sin\omega t_0. \tag{18}$$

The simple zeros of this function give place to the appearance of a critical parameter F_{cp} for which homoclinic tangles intersect, given by

$$F_{cp} = b_p \frac{2^{\frac{p}{2}}}{\pi\omega} B\left(\frac{p+2}{2},\frac{p+1}{2}\right)\cosh\left(\frac{\pi\omega}{2}\right). \tag{19}$$

The ratio $D(\omega,p) = F_{cp}/b_p$ between the critical external forcing and the damping coefficient is then

$$D(\omega,p) = \frac{2^{\frac{p}{2}}}{\pi\omega} B\left(\frac{p+2}{2},\frac{p+1}{2}\right)\cosh\left(\frac{\pi\omega}{2}\right). \tag{20}$$

One clear observation from this expression is that, for a fixed ω, the ratio of the external forcing to the damping coefficient, decreases when the damping exponent increases. This means that for higher values of the damping exponent, the critical parameter for which homoclinic chaos exist, decreases. In other words, with a smaller forcing parameter we may enter into a chaotic state, when a nonlinear damping term is considered.

C. The nonlinearly damped simple pendulum

Another paradigm in nonlinear dynamics is constituted by the simple pendulum. Analogously as in the case of the Duffing oscillator, it has been used as a practical model for many different applications in science and engineering. A generalized perturbed pendulum, including different kinds of periodic perturbations and a general damping term has been received some attention recently in [44]. As in the previous case, we consider in our model a damping term which is proportional to a power of the velocity, therefore the model equation for the nonlinearly damped simple pendulum is

$$\ddot{\theta} + b_p\dot{\theta}\left|\dot{\theta}\right|^{p-1} + \sin\theta = F\cos\omega t. \tag{21}$$

For different values of the damping exponent p, a different dissipative force is acting on the system. We consider again a very simple case of the nonlinear damping force introduced at the beginning of this paper, although there is no problem in considering the whole term, as it will be shown later.

To compute the Melnikov function associated to this system, we consider the external forcing and the nonlinear damping as a Hamiltonian perturbation to the simple pendulum with equation $\ddot{\theta} + \sin\theta = 0$. The Hamiltonian function for $(\theta,\dot{\theta}) \in [-\pi,\pi] \times R$ is

$$H(\theta,\dot{\theta}) = \frac{1}{2}\dot{\theta}^2 - \cos\theta. \tag{22}$$

The phase space of the pendulum is 2π-periodic in θ with hyperbolic saddles in ($\pm\pi$,0) and an elliptic centre in (0,0). This system has three kinds of solutions: oscillations,

rotations and a separatrix orbit. The solutions for the heteroclinic orbits can be expressed as

$$\theta_s^{\pm}(t) = \pm 2 \tanh t \ \text{sech}\ t, \tag{23}$$

$$\dot{\theta}_s^{\pm}(t) = \pm 2 \text{sech}\ t. \tag{24}$$

Thus the Melnikov function can be written as

$$M^{\pm}(t_{0,}\omega, p) = -b_p \int_{-\infty}^{+\infty} |\dot{\theta}_0^{\pm}(t)|^{p+1} dt \pm F \cos \omega t_0 \int_{-\infty}^{+\infty} \sin(\theta_0^{\pm}(t)) \dot{\theta}_0^{\pm}(t) \cos \omega t \ dt. \tag{25}$$

After substitution of the heteroclinic solutions, the evaluation of these integrals gives

$$M^{\pm}(t_{0,}\omega, p) = -b_p 2^{p+1} B\left(\frac{1}{2}, \frac{p+1}{2}\right) \pm 2\pi F \ \text{sech}\left(\frac{\pi\omega}{2}\right) \cos \omega t_0. \tag{26}$$

As a consequence of the Melnikov theory, the zeros of the Melnikov function provide the critical parameter F_{cp}, which depends on the damping exponent p, for which the stable and unstable manifolds associated to the hyperbolic saddle point intersect. In our case, this value is given by

$$F_{cp} = b_p \frac{2^p}{\pi} B\left(\frac{1}{2}, \frac{p+1}{2}\right) \cosh\left(\frac{\pi\omega}{2}\right). \tag{27}$$

Following the argumentation used in the previous cases, we define the ratio of the forcing with respect to the damping as $P(\omega, p) = F_{cp}/b_p$, and then we have the following function for the pendulum

$$P(\omega, p) = \frac{2^p}{\pi} B\left(\frac{1}{2}, \frac{p+1}{2}\right) \cosh\left(\frac{\pi\omega}{2}\right). \tag{28}$$

In this case, this ratio increases when the damping exponent p increases. That is, for higher values of the damping exponent the threshold for the homoclinic chaos to occur increases.

4. Melnikov-equivalent damped oscillators

In this section we develop the concept of Melnikov-equivalent damping, applying it to the three nonlinear oscillators we are considering throughout this work, that is, the universal escape oscillator, the Duffing oscillator and the simple pendulum. We will see that the introduction of a nonlinear damping term in a previously linearly damped oscillator may be equivalent, in the sense of Melnikov analysis, to a shift in the coefficient of the linear damping term as it was thoroughly analyzed in [19].

A. Universal escape oscillator

The previous analysis for the nonlinearly damped universal escape oscillator can be easily generalized to the case in which more powers of the velocity are included. In particular, we may find

$$\ddot{x} + \sum_{p=1}^{N} b_{p_i} \dot{x} \, |\dot{x}|^{p_i - 1} + x - x^2 = F \sin \omega t, \tag{29}$$

where N different nonlinear damping terms, with damping coefficients $b_{p_i} \geq 0$, $p_i \geq 0$, are included. The application of Melnikov analysis to this system provides a Melnikov function that takes the form

$$M^{\pm}(t_0, \omega, p_i) = -\sum_{i=1}^{N} 2 \left(\frac{3}{2}\right)^{p_i+1} b_{p_i} \, B\left(\frac{p_i + 2}{2}, p_i + 1\right) + \frac{6\pi\omega^2 F}{\sinh(\pi\omega)} \cos \omega t_0, \tag{30}$$

and consequently the critical parameter of the external perturbation is given by

$$F_{cp} = \sinh(\pi\omega) \sum_{i=1}^{N} b_{p_i} \frac{3^{p_i}}{2^{p_i+1}\pi\omega^2} B\left(\frac{p_i + 2}{2}, p_i + 1\right). \tag{31}$$

We call *generalized nonlinear damping term* to a damping term like the one we have just introduced. On the other hand, we call *simple linear damping term* to the usual linear damping term which appears in the ordinary universal escape oscillator

$$\ddot{x} + \mu\dot{x} + x - x^2 = F \sin \omega t. \tag{32}$$

Our aim here is to analyze what is the effect of the generalized nonlinear damping term with respect to the simple damping term. The analysis done above allows us to use the criterium of Melnikov equivalence, that is, *two generalized nonlinearly damped systems, having the same unperturbed differential equation, are Melnikov-equivalent if they have the same Melnikov function*. Note that the *generalized nonlinear damping term* includes the familiar nonlinear oscillator with a viscous damping term as any other version with a more complicated damping term. This criterium was introduced in [13] to study the influence of different damping models on the nonlinear roll dynamics of ships. To be precise, what we try to answer is when a nonlinear oscillator with a simple damping term is Melnikov-equivalent to a nonlinear oscillator with a generalized damping term.

The Melnikov function associated to the universal escape oscillator with a simple damping term is given by

$$M^{\pm}(t_0) = -\frac{6}{5}\mu + \frac{6\pi\omega^2 F}{\sinh(\pi\omega)} \cos \omega t_0. \tag{33}$$

Now we have two universal escape oscillators with different types of damping, one with a generalized nonlinear damping term and another one with a simple linear damping term.

We have evaluated the corresponding Melnikov functions and according to the concept of Melnikov-equivalence that we have previously introduced, we conclude that both Melnikov functions are equal when the following condition is hold

$$\mu = \frac{5}{2}\sum_{i=1}^{N}\left(\frac{3}{2}\right)^{p_i} B\left(\frac{p_i+2}{2}, p_i+1\right)\ b_{p_i}. \tag{34}$$

The meaning of this expression is the following. Given an universal escape oscillator with a nonlinear generalized damping term, in which the set of parameters (b_{p_i}, F, ω) are fixed, then there exists an universal escape oscillator with a simple linear damping term, which is Melnikov-equivalent under the following conditions: (i) The parameters F, ω are equal in both systems, and (ii) The parameter μ is related to the set of parameters b_{p_i} through Eq. (34). It is interesting to note from this result that the damping coefficient μ is a linear function of the damping coefficients b_{p_i}.

Next, we consider a particular case for which we attempt to apply this result. We consider a nonlinear universal escape oscillator including a simple linear damping term plus a cubic damping term given by the following expression

$$\ddot{x} + b_1\dot{x} + b_3\dot{x}^3 + x - x^2 = F\sin\omega t. \tag{35}$$

According to our previous result this system should be Melnikov-equivalent to the universal escape oscillator

$$\ddot{x} + \mu\dot{x} - x + x^3 = F\sin\omega t, \tag{36}$$

if the damping coefficient μ satisfies the condition

$$\mu = b_1 + \frac{18}{77}b_3. \tag{37}$$

As an easy application of Melnikov theory, we can evaluate the critical parameter $F_{cp,1}$ of the generalized nonlinearly damped universal escape oscillator from the general expression given in Eq. (31), which is

$$F_{cp,1} = \frac{1}{\pi\omega^2}\sinh(\pi\omega)\,\frac{1}{5}\left(b_1 + \frac{18}{77}b_3\right). \tag{38}$$

Analogously, the critical parameter $F_{cp,2}$ of the simple linearly damped universal escape oscillator is provided by

$$F_{cp,2} = \frac{1}{\pi\omega^2}\sinh(\pi\omega)\,\frac{1}{5}\mu. \tag{39}$$

The critical parameters that are obtained from both nonlinear oscillators are equal in the case that the condition given by Eq. (37) is fulfilled.

B. Duffing oscillator

In the case of the generalized nonlinearly damped Duffing oscillator, we have

$$\ddot{x} + \sum_{p=1}^{N} b_{p_i} \dot{x} \, |\dot{x}|^{p_i - 1} - x + x^3 = F \cos \omega t, \tag{40}$$

where N different nonlinear damping terms, with damping coefficients $b_{p_i} \geq 0$, $p_i \geq 0$, are included. The Melnikov function takes the form

$$M^{\pm}(t_0, \omega, p_i) = -\sum_{i=1}^{N} 2^{\frac{p_i+1}{2}} b_{p_i} \, B\left(\frac{p_i+2}{2}, \frac{p_i+1}{2}\right) \pm \sqrt{2} F \, \pi\omega \, \operatorname{sech}\left(\frac{\pi\omega}{2}\right) \sin \omega t_0, \tag{41}$$

and the critical parameter of the external perturbation is

$$F_{cp_i} = \cosh\left(\frac{\pi\omega}{2}\right) \sum_{i=1}^{N} \frac{2^{p_i/2}}{\pi\omega} b_{p_i} \, B\left(\frac{p_i+2}{2}, \frac{p_i+1}{2}\right). \tag{42}$$

The Melnikov function associated to the Duffing oscillator with a simple damping term,

$$\ddot{x} + \mu\dot{x} - x + x^3 = F \cos \omega t, \tag{43}$$

is given by

$$M^{\pm}(t_0) = -\frac{4}{3}\mu \pm \sqrt{2} F \, \pi\omega \, \operatorname{sech}\left(\frac{\pi\omega}{2}\right) \sin \omega t_0. \tag{44}$$

According to the concept of Melnikov-equivalence, both Melnikov functions are equal when

$$\mu = 3 \sum_{i=1}^{N} 2^{\frac{p_i-3}{2}} \, B\left(\frac{p_i+2}{2}, \frac{p_i+1}{2}\right) \, b_{p_i}, \tag{45}$$

so given a Duffing oscillator with a nonlinear generalized damping term, in which the set of parameters (b_{p_i}, F, ω) are fixed, then there exists another Duffing oscillator with a simple linear damping term, which is Melnikov-equivalent under the following conditions: (i) The parameters F, ω are equal in both systems, and (ii) The parameter μ is related to the set of parameters b_{p_i} through Eq. (45).

The particular case explored also includes a simple linear damping term plus a cubic damping term given by

$$\ddot{x} + b_1\dot{x} + b_3\dot{x}^3 - x + x^3 = F \cos \omega t. \tag{46}$$

This system is Melnikov-equivalent to the Duffing oscillator

$$\ddot{x} + \mu\dot{x} - x + x^3 = F \cos \omega t, \tag{47}$$

if μ satisfies

$$\mu = b_1 + \frac{12}{35} b_3. \tag{48}$$

The critical parameter $F_{cp,1}$ of the generalized nonlinearly damped Duffing oscillator from the general expression of Eq. (42) is given by

$$F_{cp,1} = \frac{\sqrt{2}}{\pi\omega} \cosh\left(\frac{\pi\omega}{2}\right) \left(\frac{2}{3} b_1 + \frac{8}{35} b_3\right). \tag{49}$$

And the critical parameter $F_{cp,2}$ of the simple linearly damped Duffing oscillator is

$$F_{cp,2} = \frac{\sqrt{2}}{\pi\omega} \cosh\left(\frac{\pi\omega}{2}\right) \frac{2}{3} \mu. \tag{50}$$

Both critical parameters are equal if the Eq. (48) is satisfied.

C. Simple pendulum

A similar analysis can be done for the simple pendulum. When more nonlinear damping terms are introduced the pendulum equation becomes

$$\ddot{\theta} + \sum_{i=1}^{N} b_{p_i} \dot{\theta} \left|\dot{\theta}\right|^{p_i - 1} + \sin\theta = F \cos\omega t, \tag{51}$$

which contains a generalized nonlinear damping term. The Melnikov function results in

$$M^{\pm}(t_0) = -\sum_{i=1}^{N} 2^{p_i+1} b_{p_i} \, B\left(\frac{1}{2}, \frac{p_i + 1}{2}\right) + 2\pi F \, \operatorname{sech}\left(\frac{\pi\omega}{2}\right) \cos\omega t_0, \tag{52}$$

and the critical parameter of the external perturbation is given by

$$F_{cp} = \cosh\left(\frac{\pi\omega}{2}\right) \sum_{i=1}^{N} \frac{2^{p_i}}{\pi} b_{p_i} \, B\left(\frac{1}{2}, \frac{p_i + 1}{2}\right). \tag{53}$$

The generalized nonlinearly damped pendulum is Melnikov-equivalent to the simple damped pendulum with equation

$$\ddot{\theta} + \mu\dot{\theta} + \sin\theta = F \cos\omega t, \tag{54}$$

if the amplitude F and frequency ω of the external forcing are equal in both systems, and

the parameter μ in Eq. (54) is a linear function of the set of parameters b_{p_i} given by

$$\mu = \sum_{i=1}^{N} 2^{p_i-2}\, B\left(\frac{1}{2}, \frac{p_i+1}{2}\right)\, b_{p_i}. \tag{55}$$

The particular case of the generalized damped pendulum of Eq. (51) studied here is

$$\ddot{\theta} + b_1\dot{\theta} + b_3\dot{\theta}^3 + \sin\theta = F\cos\omega t, \tag{56}$$

which is Melnikov-equivalent to the simple system of Eq. (54) if

$$\mu = b_1 + \frac{8}{3}b_3. \tag{57}$$

The critical parameter for the generalized nonlinearly damped pendulum of Eq.(56), and its associated Melnikov-equivalent simple system, is

$$F_{cp} = \frac{4}{\pi}\cosh\left(\frac{\pi\omega}{2}\right)\left(b_1 + \frac{8}{3}b_3\right). \tag{58}$$

As a summary, through the concepts of Melnikov-equivalence and of generalized nonlinear damping term, we have established a relation between different damped oscillators.

5. Energy dissipation

We have discussed in the introduction the relevance of dissipation as an ubiquitous phenomenon in physical and mechanical systems, always meaning a loss of energy due to friction forces. In this section we analyze the effect of using nonlinear damping terms on the loss of energy over a cycle and as a function of time, and the decay of the free oscillations for the nonlinear double-well Duffing oscillator. One could think, from the study done in previous sections, that the only effect that nonlinear damping terms have in the dynamics of the nonlinear oscillators is a shift in the value of the damping coefficient. In the following, we will see that this is not true because the energy dissipation of a nonlinear oscillator depends strongly on the damping term involved in the system.

In particular, we consider a nonlinear dissipative force proportional to the power of the velocity of the form

$$F_p = -b\dot{x}|\dot{x}|^{p-1}, \tag{59}$$

We consider that the damping term is small, as usually happens in applications. Then, we take the damping coefficient to be small ($b << 1$). The model equation for the nonlinearly damped Duffing oscillator reads

$$\ddot{x} + b\dot{x}|\dot{x}|^{p-1} - x + x^3 = F\cos\omega t. \tag{60}$$

Our interest now is focused in the decay of the free oscillations and how the energy

dissipates over a cycle and as a function of time, so we are interested in the unforced oscillator, that is, we fix $F = 0$ throughout this section.

One of the first consequences of the damping on a free oscillator is the decay of the amplitude of the oscillations. In order to observe and analyze this phenomenon in our case, we have numerically computed the solutions of the free nonlinearly damped Duffing oscillator for different values of the initial energy. We have numerically integrated Eq. (60) using a fourth order Runge-Kutta integrator. The temporal evolutions of the amplitude $x(t)$ are plotted in Fig.8, when $b = 0.01$, for different values of the damping exponent p and the energy E in order to visualize how the energy dissipates, and how it affects the amplitude of the oscillation. The figure shows six panels in three rows. The first row refers to the case of an orbit situated in the right well, and Fig.8(a) shows the case of dry friction, where the energy dissipates rather quickly with an apparent linear decrement setling down at the bottom of the well. We can see in Fig.8(b) for the same energy but with a cubic friction term that the energy takes longer time to decay. Note that one thing is how the energy dissipates as a function of time, and a different one is the dissipation over a cycle. Figures 8(c)-(d) show, for an orbit situated outside the well, that the amplitude decays faster for the case of dry friction than for the case of cubic friction. The last row, Fig.8(e)-(f), corresponds to the case of an orbit of higher initial energy. For $p = 0$ the energy takes longer to decay than for $p = 3$, as in the previous cases. However, in this case, for $p = 0$ the energy dissipated over a cycle for $p = 0$ is lower than

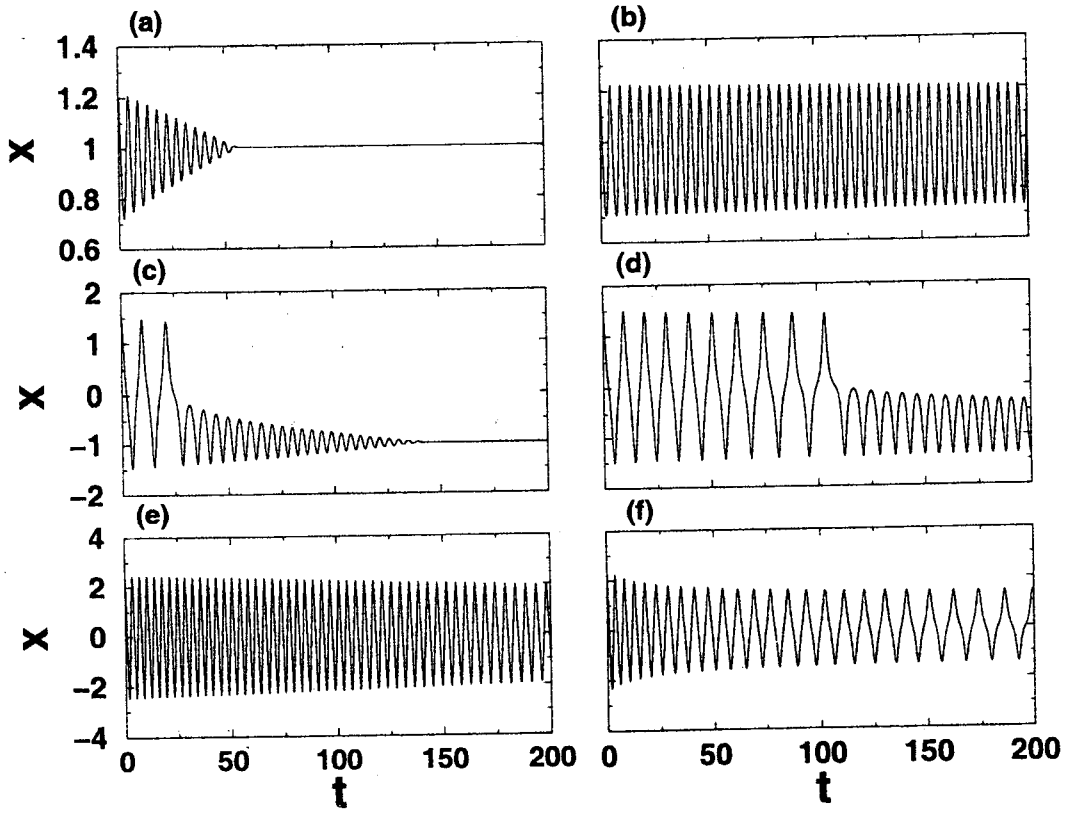

Figure 8. Decay of the amplitude of the free oscillations of the nonlinearly damped Duffing oscillator $\ddot{x} + b\dot{x}|\dot{x}|^{p-1} - x + x^3 = 0$ for different damping exponents p and different values of the initial energy ($\alpha = \sqrt{1+4E}$). (a) $p = 0$ and $\alpha = 0.5$. (b) $p = 3$ and $\alpha = 0.5$. (c) $p = 0$ and $\alpha = 1.25$. (d) $p = 3$ and $\alpha = 1.25$ (e) $p = 0$ and $\alpha = 5$. (f) $p = 3$ and $\alpha = 5$.

for $p = 3$, as we will see in the next section.

Now we are interested in evaluating how the energy dissipates over a cycle. Following the argumentation given in [9], the energy dissipated ΔE over one cycle of period T due to the damping force F_p is

$$\Delta E = \int_0^T F_p \dot{x} dt. \tag{61}$$

For simplicity during all our calculations, we define the quantity

$$\Delta_p \equiv \frac{\Delta E}{(-b)} = \int_0^T \dot{x}^2 |\dot{x}|^{p-1} dt, \tag{62}$$

where this last integral can be estimated analytically in some cases (when p is an integer), whereas otherwise numerical techniques are used. Note that, according to this expression, the evaluation of the energy dissipated over one cycle by the more general damping force considered in Eq. (1) is very easy, because it consists in the sum of several terms similar to this one. For integer values of the damping exponent p, all we need to evaluate this last integral is the amplitude $x(t)$ for the unforced and undamped oscillator and its period T. These expressions are given in Appendix B. All the necessary integrals involving Jacobian elliptic functions needed to compute these expressions have been included in the Appendix C. We have carried out analytically the computations for the energy dissipated over one cycle Δ_p for the damping exponents $p = 0,1,2,3$, which correspond to the cases of Coulomb damping, linear viscous damping, quadratic and cubic damping, respectively. All the results are displayed in Table I. In all these expressions, the parameter α is defined in terms of the energy E of the orbit as $\alpha = \sqrt{1+4E}$, and $K(m)$ and $E(m)$ are the complete elliptic integrals of the first and second kind, respectively. Information concerning Jacobian elliptic functions is found in [45]. The values of Δ_p are computed for different orbits with initial energies below the local maximum and above the local maximum, which are referred in the table as regions I and II respectively.

In Fig.9 we have plotted the analytical results for Δ_p for integer values of p increasing from $p = 0$ to $p = 3$, (solid line), and we have also included the corresponding numerical results (symbols). As is observed, the agreement between the exact solutions and the numerical computations is excellent.

After the observation of this figure, we can conclude that the energy dissipated over one cycle, Δ_p, increases as α increases for a fixed p. This can be explained if we realize that, given the dependence of the damping term with the velocity of the system (see Eq. (59)), it is obvious that the faster the system moves, the stronger the damping effect and therefore the energy dissipation is. This indicates that the energy dissipation over a period for a fixed p should increase with α, i. e., with the total energy, since the velocity of the system also increases when the total energy increases.

On the other hand, it is worth noticing how Δ_p behaves for a given α, when the damping exponent p varies. We observe that Δ_p decreases when p increases for a certain range of values of α, but it inverts its behavior when α is above a value around 1.7. The explanation of this fact can be analyzed again in terms of the damping term. We may consider two values of p, say p_1 and p_2, such that $p_1 > p_2$. It can be shown that the

Table 1. This table shows the analytical results of the energy dissipation over a cycle Δ_p for different integer values of the damping exponent p for the nonlinearly damped Duffing oscillator $\ddot{x} + b\dot{x}|\dot{x}|^{p-1} - x + x^3 = 0$. The region I indicates the region inside the double well where the initial energy of an orbit is $-1/4 < E < 0$, while the region II refers to an orbit with initial energy $E > 0$, that is, outside the double well. The parameter α is related to the initial energy E of an orbit through the relationship $\alpha = \sqrt{1+4E}$. $K(m)$ and $E(m)$ are the complete elliptic integrals of first and second kind respectively, where $0 < m < 1$ is the elliptic modulus. A plot of the energy dissipation over a cycle versus the initial energy for the different values of p considered here is represented in Fig. 9

p	Region	Δ_p
0	I	$\Delta_0 = 2\left(\sqrt{1+\alpha} - \sqrt{1-\alpha}\right)$
	II	$\Delta_0 = 4\sqrt{1+\alpha}$
1	I	$\Delta_1 = \frac{4}{3}\sqrt{\frac{1+\alpha}{2}}\left[(\alpha-1)\mathrm{K}\left(\sqrt{\frac{2\alpha}{1+\alpha}}\right) + \mathrm{E}\left(\sqrt{\frac{2\alpha}{1+\alpha}}\right)\right]$
	II	$\Delta_1 = \frac{4}{3}\sqrt{\alpha}\left[(\alpha-1)\mathrm{K}\left(\sqrt{\frac{1+\alpha}{2\alpha}}\right) + 2\mathrm{E}\left(\sqrt{\frac{1+\alpha}{2\alpha}}\right)\right]$
2	I	$\Delta_2 = \frac{4}{15}\left[(1+\alpha)^{3/2}(3\alpha-2) + (1-\alpha)^{3/2}(3\alpha+2)\right]$
	II	$\Delta_2 = \frac{8}{15}(1+\alpha)^{3/2}(3\alpha-2)$
3	I	$\Delta_3 = \frac{4}{35}\sqrt{\frac{1+\alpha}{2}}\left[(5\alpha^2-4)(\alpha-1)\mathrm{K}\left(\sqrt{\frac{2\alpha}{1+\alpha}}\right) + 4(2\alpha^2-1)\mathrm{E}\left(\sqrt{\frac{2\alpha}{1+\alpha}}\right)\right]$
	II	$\Delta_3 = \frac{4}{35}\sqrt{\frac{1+\alpha}{2}}\left[(5\alpha^2-3\alpha-4)(\alpha-1)\mathrm{K}\left(\sqrt{\frac{1+\alpha}{2\alpha}}\right) + 8(2\alpha^2-1)\mathrm{E}\left(\sqrt{\frac{1+\alpha}{2\alpha}}\right)\right]$

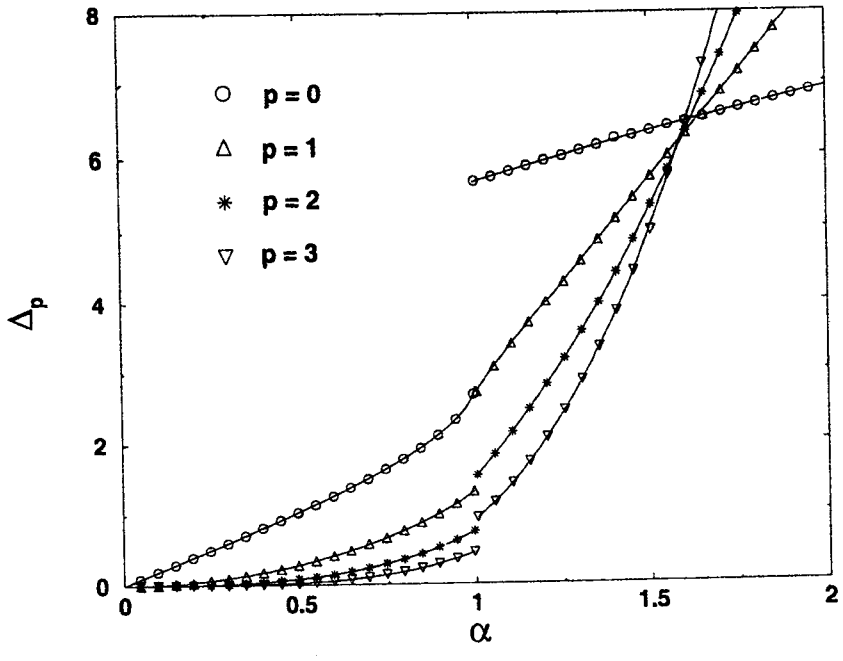

Figure 9. Dependence of the loss of the energy over a cycle Δ_p versus the initial energy ($\alpha = \sqrt{1+4E}$), for several integer values of the damping exponent p. The symbols refer to the numerical computations, whereas solid lines represent the analytical calculations. The discontinuity at $\alpha = 1$ is a manifestation of the transition from the double well to the single well above the local maximum. Notice the inversion of the behavior around the value $\alpha = \sqrt{3}$.

velocity of the orbit $\dot{x}$ is such that $|\dot{x}| < 1$ when $\alpha < \sqrt{3}$ and that only when $\alpha \geq \sqrt{3}$ the velocity is greater than 1 for some instants of time. Taking into account that the nonlinear dissipative forcing term F_p has a dependence on p given by Eq. (59), one would expect the damping effect to be weaker for p_2 than for p_1 when α is below a certain value close to $\sqrt{3}$ ($|\dot{x}| < 1$), whereas the opposite occurs when α is above this value ($|\dot{x}| > 1$). This implies that, roughly, Δ_p is a decreasing function of p for $\alpha < \sqrt{3}$ and an increasing function of p when $\alpha \geq \sqrt{3}$, which clearly corresponds to our results. Finally, the discontinuity at $\alpha = 1$ is understood if we realize that for values of $\alpha < 1$ the system is forced to move inside one of the two wells, whereas for values of $\alpha > 1$ the system has enough energy to move outside the wells. So, it is straightforward to see that a discontinuity in both the period and the velocity of the system, and therefore in Δ_p, must appear. It is interesting to note as well the gap of the curves at the discontinuity ($\alpha = 1$), which is smaller as the damping exponent p increases.

For completeness we have carried out numerical computations involving non-integer values of p. Some curves have been depicted in Figs. 10(a)-(b). In these figures, we have displayed Δ_p versus α for p ranging from 0 to 1 at intervals of 0.25 (Fig. 10(a)), and from p =1 to p = 2 with the same interval (Fig. 10 (b)). The dependence of Δ_p on α

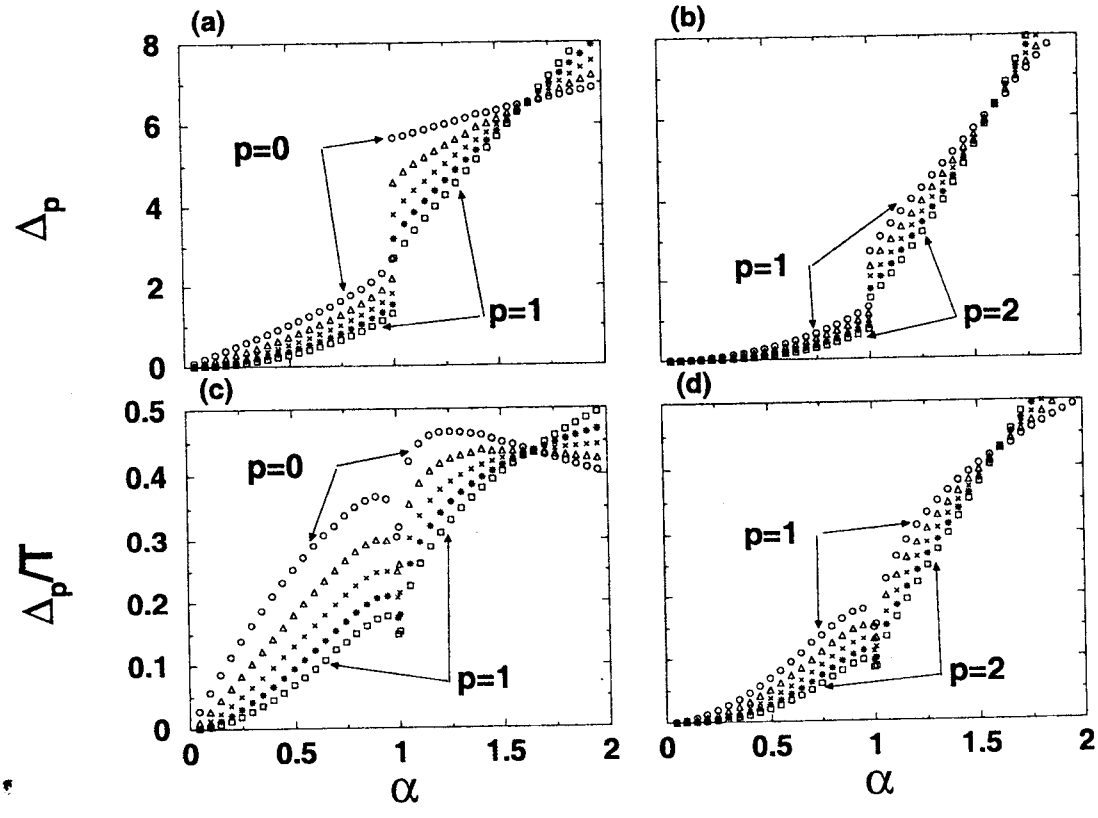

Figure 10. (a)-(b) Energy dissipation losses over a cycle for the nonlinearly damped Duffing oscillator as a function of $\alpha = \sqrt{1+4E}$ for different real values of the damping exponent p. (c)-(d) Averaged power losses over a cycle for the nonlinearly damped Duffing oscillator as a function of α for different real values of the damping exponent p. In the left panels, (a)-(c) circles stand for p = 0, triangles for p = 0.25, crosses for p = 0.5, stars for p = 0.75 and squares for p = 1. On the other hand, in the right panels (b)-(d) circles correspond to p = 1, triangles correspond to p = 1.25, crosses to p = 1.5, stars to p = 1.75 and squares to p = 2. Note that the discontinuity at α = 1 disappears for the averaged power loss Δ_p/T.

for non-integer values of p is very similar to that exhibited by the system in Fig. 9. It is worthwhile to mention here the importance of the system on the initial conditions, since it has multiple equilibria. Numerical computations for higher values of the damping exponent p show similar behavior as the one described here.

A. Energy dissipation as a function of time

The results we have described previously are not easily obtained from the temporal evolution of the amplitude of the oscillation $x(t)$ in Fig.8. For example, at first glance, one would say that the energy dissipation for $p = 0$ and $\alpha = 0.5$ (Fig. 8(a)) is stronger than for $p = 0$ and $\alpha = 5$ (Fig. 8(e)), whereas our results show that it is just the opposite. To show that our computations make sense, we have displayed in Fig. 11 some numerical estimates of the total energy of the system $E(t)$ for several values of p and α. It is clear that the behavior of $E(t)$ as a function of p and α follows that encountered for Δ_p, despite the fact that the solutions for the unforced and undamped Duffing oscillator used in the computation of Δ_p are quite different from the true trajectories shown in Fig. 8. In any case, it should be noticed that Δ_p represents in fact the loss of energy in the first cycle of the orbit, and that this dissipation of energy should be different in successive cycles. For example, in Fig. 11(c), which corresponds to $\alpha = 2$, the strongest energy loss corresponds to $p = 0$ for long values of the time variable t, whereas Δ_p is bigger for $p = 3$ than for $p = 0$,

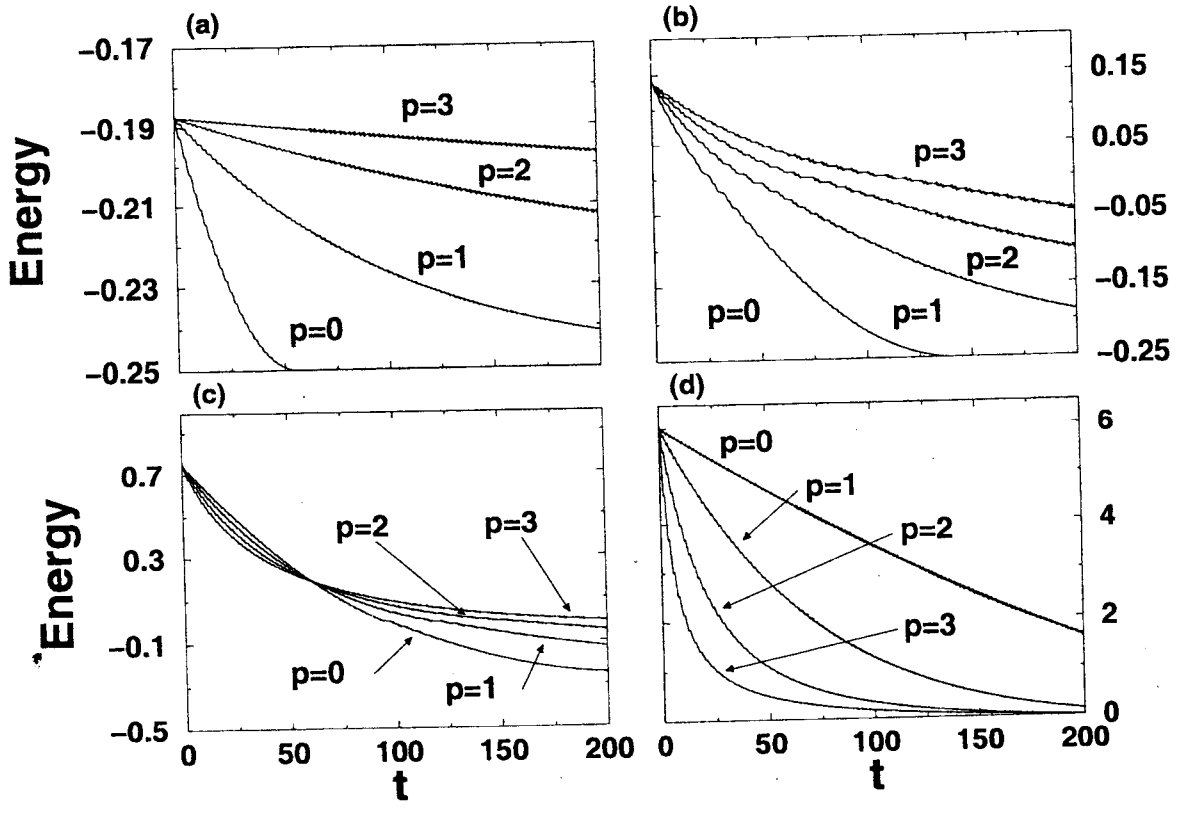

Figure 11. Total energy of the nonlinearly damped Duffing oscillator versus time for different values of p and $\alpha = \sqrt{1+4E}$. Note that the behavior of $E(t)$ follows that of Δ_p when t is not too large, as is explained in the text. (a) $\alpha = 0.5$ (b) $\alpha = 1.25$ (c) $\alpha = 2$ (d) $\alpha = 5$.

which coincides with the behavior of $E(t)$ for small values of t.

Given a dynamical system, the divergence theorem relates the volume contraction in phase space with the divergence of the flow f in the following manner [7]

$$\frac{\dot{V}(t)}{V(t)} = \text{div } f. \tag{63}$$

In the linear damping case div $f = -b$ and hence $V(t) = V_0 e^{-bt}$, which shows an exponential contraction of the volume in phase space. In a general case, for our model of nonlinear damping, we have

$$\frac{\dot{V}(t)}{V(t)} = -bp|\dot{x}|^{p-1}, \tag{64}$$

so the contraction is not exponential (note that this expression does not apply for the case $p = 0$, since the flow is discontinuous at $\dot{x} = 0$). The previous discussion is somehow related to the idea of the logarithmic decrement, which is a useful insight on the manner in which energy dissipates, defined as the natural logarithm of the ratio of the amplitudes of the oscillation on successive cycles [9] by

$$\delta_n = \ln\left(\frac{x(t+(n-1)T}{x(t+nT)}\right). \tag{65}$$

In this expression $x(t)$ is the amplitude of the oscillation in the time t, T is the period and the index n indicates the successive cycles. In the general case δ_n depends on the damping exponent p and initial energy α. However, it is well known that in the case of a harmonic oscillator with viscous damping, where the above quantity usually appears, δ_n depends only on the damping coefficient (b in Eq. (59)), but not on n nor on the initial energy.

As a method to characterize the way in which the nonlinear oscillator dissipates energy we have numerically explored the behavior of δ_n, since it gives us information about the decay of the oscillations for any general damping term. In Fig. 12, we have depicted δ_n versus n for several values of p and α. The figure shows that the logarithmic decrement depends on n (i.e., it depends on the pair of successive cycles considered) and also on the initial energy, α, and the damping exponent p. We can analyze this dependence from different points of view. A result of our analysis is that, when p is fixed, δ_1 depends on α just in the way that one would expect from the behavior of $\triangle_p$, and the same can be said when α is fixed and p changes. Moreover, by the observation of the figures it can be deduced that this analysis can be extended to δ_n when n is small enough (typically lower than 5), despite $\triangle_p$ only concerns to the first cycle ($n = 1$).

B. Power dissipation and scaling law

The definition of the energy dissipation over a cycle that we have used (Eq. (62)) shows clearly that $\triangle_p$ explicitly depends on the period T in such a way that the energy dissipation over a cycle increases as far as the period increases. This suggests that it

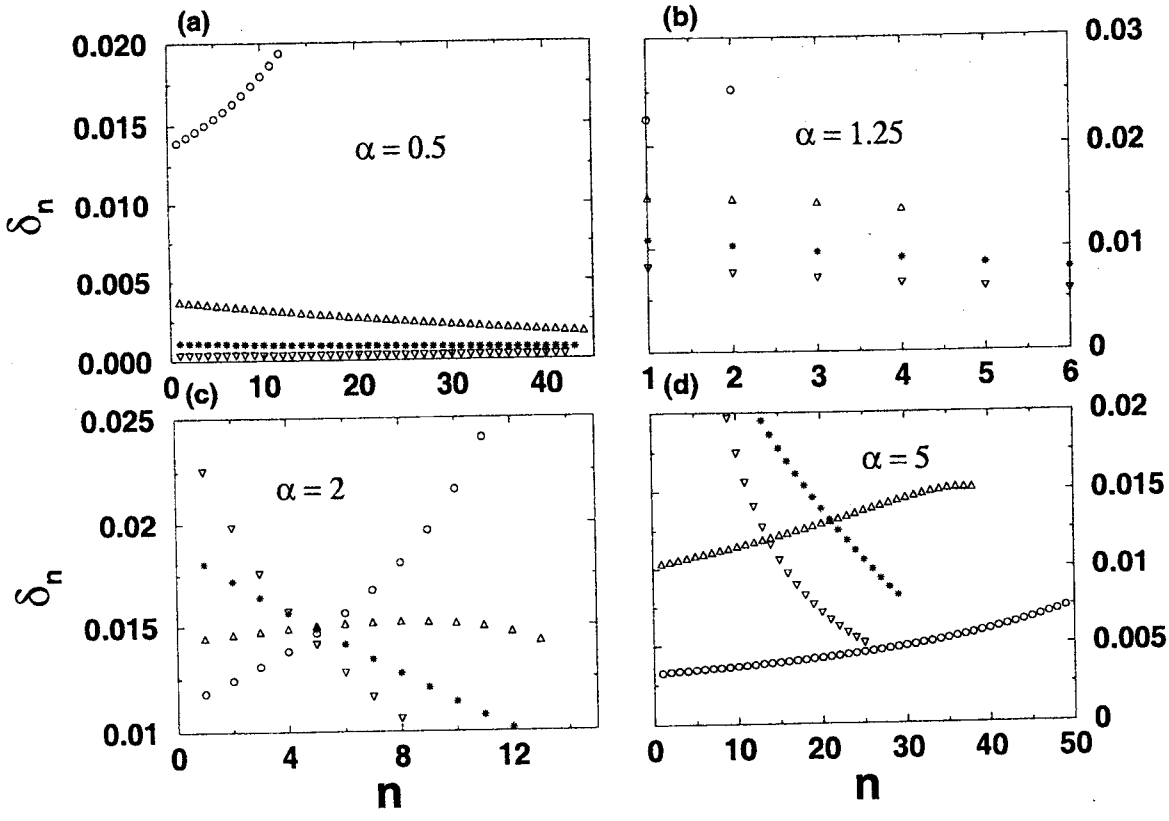

Figure 12. Logarithmic decrement for successive cycles for different values of $\alpha = \sqrt{1+4E}$ and p. The dependence on this variable is discussed in the text. The symbols have the same meaning as in Fig. 9, that is, circles stand for $p = 0$, triangles for $p = 1$, stars for $p = 2$ and inverted triangles for $p = 3$.

would be convenient to make use of a quantity independent of the duration of the cycle. For this reason, we define the *averaged power loss* in a period, $\triangle_p/T$.

We have computed this magnitude for several values of the damping exponent p, and the results of our computations are plotted in Figs. 10(c)-(d). Analogously to Fig. 10 (a)-(b), Fig. 10 (c) shows the curves for p varying from 0 to 1 at intervals of 0.25, whereas Fig. 10(d) shows the curves for p values varying in the same way but between 1 and 2, both included. Perhaps the most interesting result related to the averaged power loss in the evidence that the discontinuity at $\alpha = 1$ present in Fig. 9 for $\triangle_p$ seems to disappear here, in other words, what we have termed averaged power loss looks like a continuous function of α. We have studied the behavior of $\triangle_p/T$ for different values of the damping exponent p (analytically for integer values of p and numerically for non-integer ones), having found that $\triangle_p/T$ is in fact a continuous function of α. It should be noticed as well the presence of local maxima in the curves for both cases $\alpha < 1$ and $\alpha > 1$. In the first case, the maximum location does not change when p varies, but it does in the case $\alpha > 1$ (see Fig. 10(c), where two maxima are shown for $\alpha > 1$).

As we mentioned above, the observation of Fig.9 related to the energy dissipation $\triangle_p$ versus the energy α implies that the gap that appears at the discontinuity $\alpha = 1$ varies for the different damping exponents p. This suggest that a certain kind of scaling law should exist for $\lambda(p)$, where $\lambda(p)$ represents the gap in the discontinuity at $\alpha = 1$ for the $\triangle_p$ curves as a function of p. We have computed $\lambda(p)$ numerically for different values of

p varying from $p = 0$ to $p = 15$ (p being an integer, see Fig. 13). With the sequence we have obtained, we have applied the Aitken's method of quick convergence [46] in order to get evidence of such a scaling law. In order to apply this method to our case, we build a new sequence $d_p = \lambda(p-1) - \lambda(p)$ from the sequence of $\lambda(p)$, and afterwards define the quantity $\mu_p = d_p/d_{p+1}$. Then we analyze how μ_p behaves for increasing values of p. If μ_p tends to a constant, then a scaling law exists for $\lambda(p)$. We have found numerically that such a constant value exists and it is close to 1.48. This scaling law can also be calculated using a semi-analytical approach. If the points $(p, \lambda(p))$ are depicted in a semi-logarithmic scale, we see that the last ones (from $p = 8$ to $p = 15$) can be fitted to a straight line, i.e., they obey a decaying exponential law of the type $\lambda(p) = \lambda_0 \exp(-kp)$ where, in our case, $\lambda_0 = 1.24117$ and $k = 0.39102$. Using this expression to calculate μ_p one obtains $\mu_p = e^k = 1.478$ for all p, which is very close to the result obtained when the discrete sequence is used.

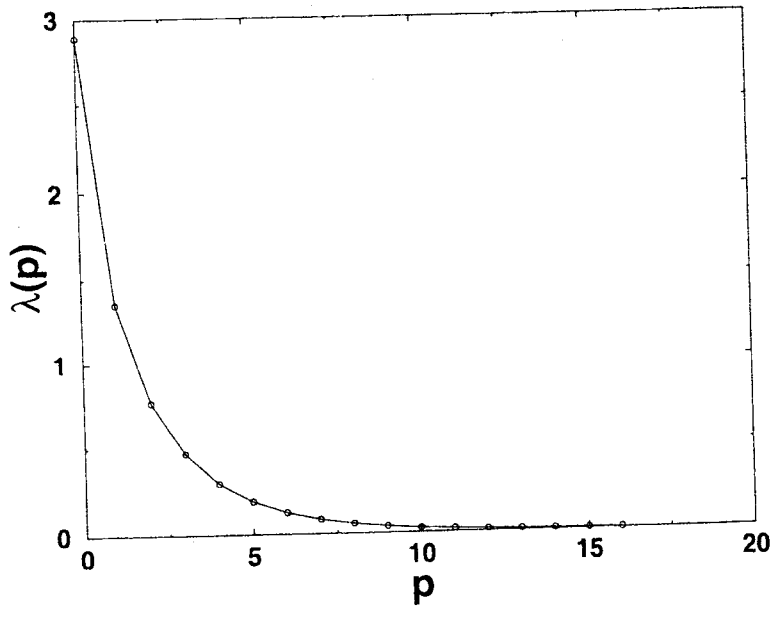

Figure 13. Value of the discontinuity of $\triangle_p$ at $\alpha = 1$ for several integer values of the damping exponents p. Symbols correspond to the numerical computations. The solid line joining the symbols is plotted as a simple visualization aid, and has no physical meaning.

6. Conclusions

As it was pointed out in the introduction, dissipation plays an important role in dynamical systems, and in many problems related to Sound and Vibration Engineering. In spite of the enormous efforts to analyze these systems, very few works appear to exist, in which nonlinear dissipation is considered. As a matter of fact, it seems that the effect of nonlinear dissipation on certain nonlinear dynamical systems has been missed or underestimated.

In the case of the universal escape oscillator, we have analyzed how the introduction of nonlinear damping terms affects the threshold of the period-doubling bifurcation route to chaos, the boundary crises leading to final escape to infinity and the

threshold parameter for the appearance of the fractal basin boundaries. Moreover, the effect of using different nonlinear damping terms on the erosion of the nonescaping basins has been extensively studied. Our numerical observations suggest that the increase of the damping exponent has similar effects as the decrease suggest that the increase of the damping exponent has similar effects as the decrease of the damping level for a linearly damped model.

We have analyzed the universal escape oscillator, the Duffing oscillator and the simple pendulum, with nonlinear damping terms proportional to the power of the velocity. The threshold parameters for which homoclinic or heteroclinic chaos is expected, have been analytically computed using the Melnikov method. Our analysis has provided some useful general expressions which can be of application to various models in science and technology, where nonlinear damping terms proportional to the power of the velocity are included. Using the concept of Melnikov equivalence and the generalized nonlinear damping term, which includes several nonlinear damping terms, we have shown that the effect of nonlinear dissipation can be equivalent to a linearly damped nonlinear oscillator with a modified damping coefficient.

On the other hand, the energy dissipation of a nonlinearly damped Duffing oscillator with a dissipative term proportional to the power of the velocity has been analyzed in detail. The presence of a discontinuity at the value of $\alpha = \sqrt{1+4E} = 1$ and an inversion of the behavior of $\triangle_p$ for values of the energy above $\alpha \simeq \sqrt{3}$ have been studied and explained in terms of the dynamical behavior of the model. These results are contrasted with the evolution of the energy dissipation as a function of time for different values of the damping exponent p and initial energy α, finding that the dependence on these parameters for small values of time t is coherent with the results found for the dissipation of the energy $\triangle_p$. In order to avoid the dependence of the energy dissipation on the period, we have defined an averaged power loss in a period. The information provided by this new magnitude is rather similar to the one provided by the energy dissipation over a cycle, although no discontinuity is present in this case. As a usual tool in the study of the decay of the oscillations, we have also computed the logarithmic decrement of the system for different values of p and α, having obtained consistence with our previous results and some resemblances with the harmonic oscillator when $p = 1$. Finally the discontinuity gap which appears for the energy dissipation at $\alpha = 1$, has been investigated with the result that this gap decreases as the power of the damping term increases. The analysis of the sequence of gaps for different damping exponents p has shown the presence of a scaling law associated with this dependence.

As a summary, we would like to stress the fact that besides this detailed overview of the effects of nonlinear damping of the behavior on nonlinear oscillators, further work is needed in this direction which might give light in the complexities of friction and its dynamical consequences. Precisely the simplicity of the models, makes it a fruitful area with many possible applications in science and technology.

Acknowledgements

We have benefited from discussions about this work with B. Balachandran, L.N. Virgin, E. Barreto and Ulrich Parlitz. This work has been supported by the Spanish DGES under project PB96-0123, and the Spanish Ministry of Science and Technology

under project BFM2000-0967.

Appendix A. Useful integrals

Integrals used for the computation of Melnikov functions are:

$$\int_{-\infty}^{+\infty} dt\, \frac{\sinh^{\mu}(t)}{\cosh^{\nu}(t)} = B\left(\frac{\mu+1}{2}, \frac{\nu-\mu}{2}\right) \tag{A.1}$$

$$\int_{-\infty}^{+\infty} dt\, \operatorname{sech} At \cos Bt = \frac{\pi}{A}\operatorname{sech}\left(\frac{\pi B}{2A}\right) \tag{A.2}$$

$$\int_{-\infty}^{+\infty} dt\, \operatorname{sech} At \tanh At \sin Bt = \frac{\pi B}{A^2}\operatorname{sech}\left(\frac{\pi B}{2A}\right) \tag{A.3}$$

The Euler Beta functions are related to the Gamma Euler Function through the expression:

$$B(r,s) = \frac{\Gamma(r)\Gamma(s)}{\Gamma(r+s)}. \tag{A.4}$$

Remember that the Euler Gamma function has the following property: $\Gamma(n+1) = n\Gamma(n)$, where $\Gamma(n+1) = n!$, $0! = 1$, if $n = 0,1,2,\ldots,$ and $\Gamma(1/2)=\sqrt{\pi}, \Gamma(n+1/2) = \frac{1\cdot 3\cdot 5\cdot\ldots\cdot(2n-1)}{2^n}\sqrt{\pi}$.

Appendix B. Analytical solutions of the Duffing oscillator

We want to explicitly obtain the exact solutions for the double-well Duffing oscillator

$$\ddot{x} - x + x^3 = 0. \tag{B.1}$$

Our objective is to look for analytical expressions for the solutions and the period of the motions of the system. We have two different kind of motions depending on the energy of the orbit. There is a motion inside a well, for values $-1/4 < E < 0$, where the solution of the period is given by

$$T(\alpha) = \frac{2\sqrt{2}}{\sqrt{1+\alpha}}\,\mathrm{K}\left(\sqrt{\frac{2\alpha}{1+\alpha}}\right), \tag{B.2}$$

where $K(m)$ is the *complete elliptic integral of first kind* [45], and m is the elliptic modulus. Inside one of the small well $-1/4 < E < 0$ and consequently $0 < \alpha < 1$, and the elliptic modulus m satisfies the condition $0 < m < 1$, as expected.

The exact solution for an orbit in this region is given by

$$x(t) = \sqrt{\alpha+1}\,\mathrm{dn}\left(\sqrt{\frac{\alpha+1}{2}}t, \sqrt{\frac{2\alpha}{\alpha+1}}\right), \tag{B.3}$$

where $\alpha = \sqrt{1+4E}$ and $-\frac{1}{4} < E < 0$.

The period of an orbit for energies $E > 0$ is given by

$$T(\alpha) = \frac{4}{\sqrt{\alpha}} \mathrm{K}\left(\sqrt{\frac{1+\alpha}{2\alpha}}\right), \tag{B.4}$$

where as $E > 0$, then $\alpha > 1$, and consequently m satisfies the condition $1/\sqrt{2} < m < 1$. The exact solution for an orbit in this region is given by

$$x(t) = \sqrt{\alpha+1}\ \mathrm{cn}\left(\sqrt{\alpha}t, \sqrt{\frac{\alpha+1}{2\alpha}}\right) \tag{B.5}$$

where $\alpha = \sqrt{1+4E}$ and $E > 0$.

Appendix C. List of integrals involving elliptic functions

We include a list of integrals that have been used in this work, based in [45]. In the list, sn(x,m), cn(x,m) and dn (x,m) are the Jacobian elliptic functions, and K(m) and E(m) are the complete elliptic integrals of the first and second kind, respectively.

$$\int_0^{4K(m)} \mathrm{dn}^2(x,m)dx = 4\mathrm{E}(m), \tag{C.1}$$

$$\int_0^{4K(m)} \mathrm{dn}^4(x,m)dx = \frac{4}{3}\left((m^2-1)\mathrm{K}(m) + 2(2-m^2)\mathrm{E}(m)\right), \tag{C.2}$$

$$\int_0^{4K(m)} \mathrm{dn}^6(x,m)dx = \frac{4}{15}\left(4(2-m^2)(m^2-1)\mathrm{K}(m) + (8m^4-23m^2+23)\mathrm{E}(m)\right), \tag{C.3}$$

$$\int_0^{4K(m)} \mathrm{dn}^8(x,m)dx = \frac{4}{7}\left(\frac{5}{3}(1-m^2) - \frac{8}{5}(2-m^2)^2\right)(1-m^2)\mathrm{K}(m) \tag{C.4}$$

$$+ \frac{4}{7}\left(\frac{2}{5}(8m^4-23m^2+23) - \frac{10}{3}(1-m^2)\right)(2-m^2)\mathrm{E}(m), \tag{C.5}$$

$$\int \mathrm{sn}(x,m)\mathrm{cn}(x,m)dx = -\frac{1}{m^2}\mathrm{dn}(x,m), \tag{C.6}$$

$$\int \mathrm{sn}(x,m)\mathrm{dn}(x,m)dx = -\mathrm{cn}(x,m). \tag{C.7}$$

References

1. J. Mawhin, "The forced pendulum: A paradigm for nonlinear analysis and dynamical systems, Exp. Math. **6** (1998) 271-287.
2. F. C. Moon, Chaotic and Fractal Dynamics. An introduction for Applied Scientists and Engineers, Wiley, New York, 1992.
3. S. Aubry. "The concept of anti-integrability applied to dynamical systems and to structural and electronic models in condensed matter physics", Physica D **71** (1994) 196.

4. J. Wisdom. "Chaotic behavior in the Solar_System", Proc. R. Soc. Lond. A **413** (1987) 109.
5. J. D. Murray, Mathematical Biology, Springer-Verlag, New York, Third edition, 2001.
6. P. W. Anderson, K. J. Arrow and D. Pines (Eds). The Economy as an Evolving Complex System. Addison-Wesley, New York, 1998.
7. L. N. Virgin, Introduction to Experimental Nonlinear Dynamics, Cambridge University Press, Cambridge, 2000.
8. B. Feeny and A. Guran, "Friction as a nonlinearity in Dynamics: A historical review" in *Nonlinear Dynamics*, (ed. A. Guran), World Scientific, Singapore, 1997.
9. S. G. Kelly, Fundamentals of Mechanical Vibrations, McGraw-Hill, New York, 1993.
10. B. Ravindra, and A. K. Mallik, "Stability analysis of a non-linearly damped Duffing oscillator", J. Sound Vibration **171** (1994) 708-716.
11. B. Ravindra, and A. K. Mallik, "Role of nonlinear dissipation in soft Duffing oscillators", Phys. Rev. E **49** (1994) 4950-4954.
12. B. Ravindra, and A. K. Mallik, "Chaotic response of a harmonically excited mass on an isolator with non-linear stiffness and damping characteristics", J. Sound Vibration **182** (1995) 345-353.
13. M. Bikdash, B. Balachandran, and A. Nayfeh, "Melnikov analysis for a ship with a general roll-damping model", Nonlinear Dynamics **6** (1994) 101-124.
14. J. M. Falzarano, S.W. Shaw, and A.W. Troesch, "Application of global methods for analyzing dynamical systems to ship rolling motion and capsizing", Int. J. Bifurcation and Chaos **2** (1992) 101-1154.
15. H. S. Y. Chan, Z. Xu, and W. L. Huang, "Estimation of nonlinear damping coefficients from large-amplitude ship rolling motions", Applied Ocean Research **17** (1995) 217-224.
16. N. De Mestre, The Mathematics of Projectiles in Sport, Cambridge University Press, Cambridge, 1990.
17. R. R. Huilgol, J. R. Christie, and M. P. Panizza, "The Motion of a Mass Hanging from an Overhead Crane", Chaos, Solitons and Fractals **5** (1995) 1619-1631.
18. M. A. F. Sanjuán, "The effect of nonlinear damping on the universal escape oscillator", Int. J. Bifurcation and Chaos **9** (1999) 735-744.
19. J. L. Trueba, J. Rams and M. A. F. Sanjuán, "Analytical estimates of the effect of nonlinear damping in some nonlinear oscillators", Int. J. Bifurcation and Chaos **10** (2000) 2257-2267.
20. J. P. Baltanás, J. L. Trueba and M. A. F. Sanjuán, "Energy dissipation in a nonlinearly damped Duffing oscillator", Physica D, to appear (2001).
21. D. Pfenniger, and C. Norman, "Dissipation in barred galaxies: The growth of bulges and central mass concentrations", The Astrophysical Journal **363** (1990) 391-410.
22. J. Binney, and S. Tremaine, Galactic Dynamics, Princeton University Press, Princeton, 1987.
23. M. A. F. Sanjuán, "Remarks on transitions Order-chaos Induced by the Shape of the Periodic Excitation in a Parametric Pendulum", Chaos, Solitons and Fractals **7** (1996) 435-440.
24. M. A. F. Sanjuán, "Subharmonic bifurcations in a pendulum parametrically excited by a nonharmonic perturbation", Chaos, Solitons and Fractals **9** (1998) 995-1003.
25. M. A. F. Sanjuán, "Using nonharmonic forcing to switch the periodicity in nonlinear systems", Phys. Rev. E **58** (1998) 4377-4382.
26. M. A. F. Sanjuán, "Comments on the Hamiltonian formulation for linear and non-linear oscillators including dissipation", J. Sound Vib. **185** (1995) 734-736.
27. M. A. F. Sanjuán, "Homoclinic bifurcations sets of driven nonlinear oscillators", Int. J. Theor. Phys. **35** (1996) 1745-1752.
28. J. A. Gottwald, L. N. Virgin, and E. H. Dowell "Routes to escape from an energy well", J. Sound and Vibration **187** (1995) 133-144.
29. J. M. T. Thompson, S. R. Bishop & L. M. Leung, "Fractal basins and chaotic bifurcations prior to escape from a potential well", Physics Letters A **121** (1987) 116-120.
30. J. M. T. Thompson, "Chaotic phenomena triggering the escape from a potential well", Proc. Roy. Soc. Lond. **A421** (1989) 195-225.
31. J. M. T. Thompson, "Fractal control boundaries of driven oscillators and their relevance to safe engineering design", Proc. Roy. Soc. Lond. A **428** (1990) 1-13.
32. M. S. Soliman and J. M. T. Thompson, "Basin organization prior to a tangled saddlenode

bifurcation", Int. J. Bifurcation and Chaos **1** (1991) 107-119.
33. M. S. Soliman and J. M. T. Thompson, "The effect of damping on the steady state and basin bifurcation patterns of a nonlinear mechanical oscillator", Int. J. Bifurcation and Chaos **2** (1992) 81-91.
34. M. S. Soliman, "Predicting regimes of indeterminate jumps to resonance by assessing fractal boundaries in control space", Int. J. Bifurcation and Chaos **4** (1994) 1645-1653.
35. K. T. Alligood, T. D. Sauer, and J. A. Yorke, Chaos: An Introduction to Dynamical Systems, (Springer, New York, Third printing, pp. 203-207, 2001
36. H. E. Nusse and J. A. Yorke, "Basins of attraction", Science **271** (1996) 1376-1380.
37. H. E. Nusse, E. Ott and J. A. Yorke, "Saddle-Node Bifurcations on Fractal basin boundaries", Phys.Rev. Lett. **75** (1995) 2482-2485.
38. H. E. Nusse and J. A. Yorke, "Wada basin boundaries and basin cells", Physica D **90** (1996) 242-261.
39. H. E. Nusse and J. A. Yorke, "Fractal basin boundaries generated by basin cells and the geometry and mixing chaotic flows", Phys. Rev. Lett **84** (2000) 626-629.
40. S. Wiggins, Introduction to Applied Nonlinear Dynamical Systems and Chaos, Springer-Verlag, Berlin, 1990.
41. Y. Ketema, "A physical interpretation of Melnikov's method", Int. Journal of Bifurcation and Chaos **2** (1992) 1-9.
42. F. C. Moon and G.-X. Li, "Fractal basin boundaries and homoclinic orbits for periodic motions in a two-well potential", Phys. Rev. Lett. **55** (1985) 1439-1442.
43. A. Abramowicz, and I. Stegun, Handbook of Mathematical Functions, Dover, New York, 1970.
44. J. L.Trueba, J. P. Baltanás and Miguel A. F. Sanjuán, "A generalized perturbed pendulum". Submitted to Chaos, Solitons & Fractals, (2001).
45. D. Lawden, Elliptic Functions and Applications, Springer-Verlag, Berlin, 1989; L. M. Milne-Thomson, in *Handbook of Mathematical Functions*, (eds. A. Abramowitz and I. Stegun), Dover, New York, 1970.
46. W. H. Press, S. A. Teukolsky, W. T. Vetterling, and B. P. Flannery, Numerical Recipes in C, Cambridge University Press, Cambridge, 1992.